

# Temporomandibular joint shape in anthropoid primates varies widely and is patterned by size and phylogeny

Claire E. Terhune<sup>1</sup>  | D. Rex Mitchell<sup>2</sup>  | Siobhán B. Cooke<sup>3,4</sup>  |  
 Claire A. Kirchhoff<sup>5</sup>  | Jason S. Massey<sup>6</sup> 

<sup>1</sup>Department of Anthropology, University of Arkansas, Fayetteville, Arkansas, USA

<sup>2</sup>College of Science and Engineering, Flinders University, Adelaide, South Australia, Australia

<sup>3</sup>Center for Functional Anatomy and Evolution, Johns Hopkins University School of Medicine, Baltimore, Maryland, USA

<sup>4</sup>New York Consortium in Evolutionary Primatology Morphometrics Group, New York, New York, USA

<sup>5</sup>Department of Biomedical Sciences, Marquette University, Milwaukee, Wisconsin, USA

<sup>6</sup>Department of Anatomy and Developmental Biology, Biomedicine Discovery Institute, Monash University, Melbourne, Victoria, Australia

## Correspondence

Claire E. Terhune, Department of Anthropology, University of Arkansas, 330 Old Main, Fayetteville, AR 72701, USA.

Email: [cterhune@uark.edu](mailto:cterhune@uark.edu)

## Funding information

National Science Foundation, Grant/Award Numbers: BCS-1551669, BCS-1551722, BCS-1551766

## Abstract

The temporomandibular joint is the direct interface between the mandible and the cranium and is critical for transmitting joint reaction forces and determining mandibular range of motion. As a consequence, understanding variation in the morphology of this joint and how it relates to other aspects of craniofacial form is important for better understanding masticatory function. Here, we present a detailed three-dimensional (3D) geometric morphometric analysis of the cranial component of this joint, the glenoid fossa, across a sample of 17 anthropoid primates, and we evaluate covariation between the glenoid and the cranium and mandible. We find high levels of intraspecific variation in glenoid shape that is likely linked to sexual dimorphism and joint remodeling, and we identify differences in mean glenoid shape across taxonomic groups and in relation to size. Analyses of covariation reveal strong relationships between glenoid shape and a variety of aspects of cranial and mandibular form. Our findings suggest that intraspecific variation in glenoid shape in primates could further be reflective of high levels of functional flexibility in the masticatory apparatus, as has also been suggested for primate jaw kinematics and muscle activation patterns. Conversely, interspecific differences likely reflect larger scale differences between species in body size and/or masticatory function. Results of the covariation analyses dovetail with those examining covariation in the cranium of canids and may be indicative of larger patterns across mammals.

## KEYWORDS

covariation, geometric morphometrics, glenoid, masticatory apparatus

## 1 | INTRODUCTION

The temporomandibular joint (TMJ), as the bony connection between the mandible and the cranium, is critical for transmitting joint reaction forces and for determining mandibular range of motion, which itself can be tied to dietary differences and ecological niche (e.g., Terhune, Cooke, & Otárola-Castillo, 2015). Because of the importance of this

joint for masticatory function, shape of the TMJ is likely under strong selection to optimize masticatory function while minimizing injury and/or the occurrence of pathologies. Yet, the range of intraspecific variation in TMJ form remains almost entirely unexplored (but see Osborn & Baragar, 1992), and while interspecific shape variation has been examined in some primates (e.g., Ashton & Zuckerman, 1954; Terhune, 2011a, 2013a; Vinyard, 1999;

Vinyard et al., 2003; Wall, 1995, 1997, 1999), large-scale analyses of three-dimensional (3D) shape have yet to be undertaken, and even fewer have attempted to look at covariation between TMJ shape and other aspects of the craniofacial skeleton.

Characterizing the range of variation within and between primate species may provide important clues regarding TMJ plasticity, may be reflective of the breadth of a given species' dietary niche, and may suggest functional differences in the masticatory apparatus in relation to sexual selection (Terhune et al., 2015). Across taxa, analyses of TMJ shape variation may reveal patterns of selection related to masticatory behaviors and/or diet or may point to differences in non-masticatory behaviors such as canine displays or vocalization. Equally critically, how the shape of the TMJ covaries with other aspects of the masticatory apparatus, such as overall cranial and/or glenoid shape, may reveal important biomechanical tradeoffs in masticatory form and function that have not been previously identified. The goal of the research presented here is to quantify 3D TMJ shape, as represented by the glenoid fossa, across a large sample of anthropoid primates, and especially to examine how shape variation is patterned within and among species in relation to size and phylogeny, and how glenoid shape covaries with cranial and mandibular shape. This will provide important context for future and ongoing studies of covariation within the masticatory apparatus and studies of dental morphology and wear, as well as pathology rates and/or trauma in the masticatory system and TMJ.

## 1.1 | TMJ anatomy and function

The TMJ is a complex joint composed of upper and lower joint compartments with a fibrocartilaginous articular disc interposed between the mandibular condyle and glenoid fossa (Figure 1); compounding this complexity is that both the left and right TMJs must work in concert to generate mandibular movements. Indeed, movements at this joint are intricate; with the mandible at rest (i.e., centric relation), the condyle is situated on the posterior slope of the articular eminence (AE) of the glenoid (mandibular) fossa (Turp et al., 2008). During jaw opening movements, the anteroposteriorly (AP) convex condyle slides inferiorly and anteriorly along the AP convex AE and onto the preglenoid plane of the glenoid fossa. This sagittal sliding (Wall, 1999) results from a combination of condylar translation and rotation. Though the condyle and AE are largely non-congruent, AP length and curvature of these articular surfaces has been linked to sagittal sliding and increased maximum jaw gape (Terhune, 2011a, 2013a; Terhune et al., 2015; Wall, 1999). During mastication,

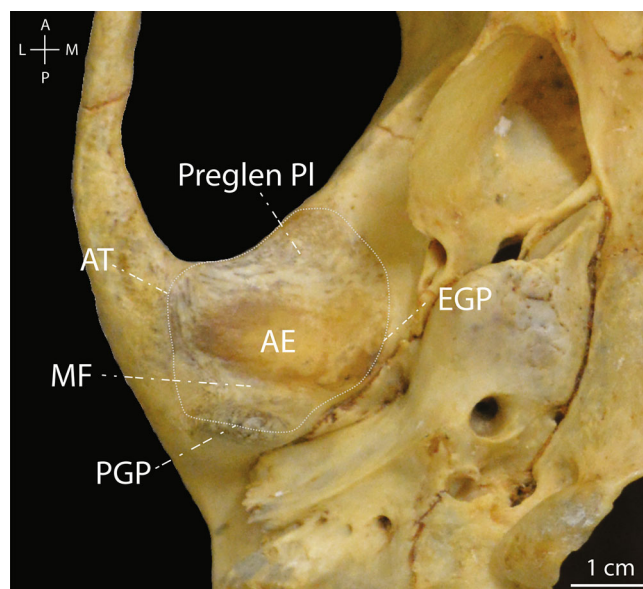


**FIGURE 1** Inferior view of the right glenoid fossa of a male *Macaca fascicularis* (NMNH 197662) showing relevant anatomical features and glenoid articular surface outline. AE, articular eminence; AT, articular tubercle; EGP, entoglenoid process; MF, mandibular fossa; PGP, postglenoid process; Preglen PI, preglenoid plane. Anatomical directions: A, anterior, P, posterior, M, medial, L, lateral

sagittal sliding is combined with lateral deviation of the mandible, where the working-side (chewing) condyle rotates on the posterior slope of the AE and moves slightly laterally, while the balancing-side (non-chewing) condyle slides anteriorly onto the peak of the AE and/or the preglenoid plane (Hylander, 2006). Two processes in the joint, the entoglenoid process (EGP; situated on the medial margin of the joint) and the postglenoid process (PGP; situated on the posterior aspect of the joint) are thought to act as bony guides for movements of the condyle during both masticatory and non-masticatory movements (e.g., Wall, 1995, 1999). The EGP especially has been demonstrated to have direct contact with the mandibular condyle during mastication (Wall, 1999), and wide/projecting EGPs are suggested to guide sagittal sliding and limit mediolateral movements of the condyle. The role of the PGP is less clear as the condyle is largely buffered from direct contact with the PGP by the articular disc (e.g., Hylander, 2006), though it is likely it also functions as a bony stop on posterior movements of the condyle. Flatter, less convex joints with less projecting processes have been hypothesized (Hylander, 1979, 1988; Terhune, Cooke, & Otárola-Castillo, 2015; Wall, 1999) to be linked to less congruence between the condyle and glenoid and, therefore, increased joint range of motion (and perhaps less precise occlusion during jaw closing), while joints with more topographic relief have been suggested to

display increased glenoid/condyle congruence and more limited range of motion (with corresponding increases in occlusal precision).

Much of our understanding of masticatory variation and function is based on comparative (e.g., Ashton & Zuckerman, 1954; Endo et al., 2011; Hinton, 1981, 1983; Moffett et al., 1964; Nickel et al., 1988; Öberg et al., 1971; Yamada et al., 2004) and experimental (e.g., Baragar & Osborn, 1984, 1987; Bennett, 1908; Ferrario et al., 2005; Gallo et al., 1997, 2000; Grant, 1973; Miyawaki et al., 2000, 2001) studies of modern humans. However, the shape of the human masticatory apparatus and TMJ is unique (e.g., reduced facial prognathism, an extremely pronounced AE, and a reduced PGP), and there is considerable variation across primates (Bouvier, 1986a, 1986b; Lockwood et al., 2002; Smith et al., 1983; Terhune, 2010, 2011a, 2011b, 2013a, 2013b; Vinyard, 1999; Vinyard et al., 2003; Wall, 1999). Like the dentition, variation in bony morphology of the cranium and mandible, including the TMJ, has also been linked to differences in feeding behavior among primate taxa. In the TMJ, some features have been linked to feeding behavior in primates (e.g., Bouvier, 1986a, 1986b; Smith et al., 1983; Taylor, 2005; Terhune, 2011a, 2011b, 2013a; Vinyard, 1999; Vinyard et al., 2003; Wall, 1995, 1999). For example, AE shape is likely a consequence of height of the TMJ above the occlusal plane, which itself is linked to increased dietary resistance (Terhune, 2011b). Further, increased anteroposterior curvature of the condyle and AP elongated preglenoid planes have been suggested to facilitate increased jaw gapes (Terhune, 2011a, 2013a). Overall, the emerging pattern of morphological variation seems to suggest that TMJ morphology can be more consistently linked to mandibular range of motion than force production (e.g., Terhune, 2011a, 2011b, 2013a, 2013b; Terhune, Hylander, et al., 2015; Vinyard et al., 2003; Wall, 1999). However, the relationship between diet and bony morphology tends to be less straightforward compared to dental morphology, and studies provide conflicting results (Vinyard et al., 2011).

Some aspects of the TMJ have also been previously identified to vary in relation to size and phylogeny. The majority of TMJ scaling analyses (i.e., Bouvier, 1986a, 1986b; Smith et al., 1983; Vinyard, 1999) analyzed only condylar shape, and all came to slightly different conclusions regarding anthropoid (Bouvier, 1986a, 1986b; Smith et al., 1983) and strepsirrhine (Vinyard, 1999) scaling relative to body mass and/or mandible length. Generally, they found that aspects of condyle shape (i.e., condyle width or length) scaled either with isometry or positive allometry. Only Terhune (2017) examined scaling of both glenoid and condylar shape across a large sample of anthropoids. This analysis used both traditional and

geometric morphometric approaches and also incorporated phylogeny into the statistical analyses. Results indicated that most features had a strong phylogenetic signal and did indeed scale with isometry or positive allometry relative to body mass and/or mandible length, though several features (height of the TMJ above the occlusal plane, condylar area) displayed a different scaling pattern in male cercopithecoids, perhaps related to canine display behaviors. The geometric morphometric analyses revealed that, while craniofacial and masticatory shape were strongly allometric, glenoid shape alone was less consistently allometrically patterned. Notably, however, this prior analysis only looked at species averages and used fixed 3D landmarks on the cranium (59 landmarks total) or glenoid (12 landmarks); therefore, it was unable to fully capture some aspects of glenoid and cranial shape variation.

One major factor that likely contributes to TMJ shape variation is remodeling, which occurs throughout the lifetime of an individual. Histological, comparative, and clinical studies of TMJ morphology have linked age and changes in dental function to altered joint form (Granados, 1979; Hinton, 1981; Jasinevicius et al., 2006; Kurita et al., 2000; Moffett et al., 1964; Richards, 1988; Yamada et al., 2004). The majority of these studies suggest that, at least in humans, the AE undergoes remodeling with dental wear and the eminence and condyle gradually flatten with age. Additionally, multiple analyses (Bouvier, 1986a, 1986b; Hylander, 1979; Hylander & Bays, 1979) suggest that forces are highest in the lateral aspect of the joint, and a higher occurrence of disc perforations and osteoarthritic lesions occur in this region (i.e., Öberg et al., 1971; Richards & Brown, 1981). Some researchers have further concluded that gradual flattening of the eminence may be a precursor to articular disc displacement or “clicking” in the TMJ. Although limited, studies of nonhuman primate TMJ remodeling further support the conclusion that TMJ form is plastic and that remodeling of this joint continues to occur well into adulthood in response to altered dental function and other perturbations of the masticatory apparatus (e.g., Hinton & McNamara, 1984; Matsuka et al., 1998). At present, the extent to which remodeling of the glenoid fossa and condyle alters joint contours throughout adulthood in nonhuman primates is unclear, and we especially lack data on how changes in joint form may be linked to dental function.

## 1.2 | Research objectives

Here, we quantify glenoid fossa shape broadly across anthropoid primates with the goal of examining both intra and interspecific shape variation. We especially focus on the latter and examine how

shape variation is patterned phylogenetically and allometrically.

We first ask the research question: How do anthropoid taxa differ in glenoid fossa shape? Prior research suggests that TMJ morphology is phylogenetically patterned across primates, but none have systematically documented shape variation across a wide range of species or between sexes within species. Additionally, no prior analyses have examined the detailed 3D shape of the entire joint surface, which we do here for the first time. As part of this, we examine how average glenoid shape for each species/sex is patterned in relation to phylogeny and body and/or cranial size.

Our second research question asks: How does glenoid fossa shape covary with cranial and mandibular shape across species? Prior research has focused on examining components of the masticatory apparatus and overall cranial shape in isolation, but by necessity, the components of the masticatory apparatus and skull must work in conjunction with one another during both masticatory and non-masticatory behaviors (i.e., speech/vocalization, display behaviors). Therefore, we combine these often separately analyzed datasets and ask how shape variation in one region (e.g., the mandible) may relate to aspects of the glenoid fossa (and vice versa).

## 2 | MATERIALS AND METHODS

### 2.1 | Samples

This study included data from 918 individuals from 17 taxa of nonhuman anthropoid primates (Figure 2). We elected to exclude humans from our analysis because the shape of their TMJ is so divergent from other anthropoid

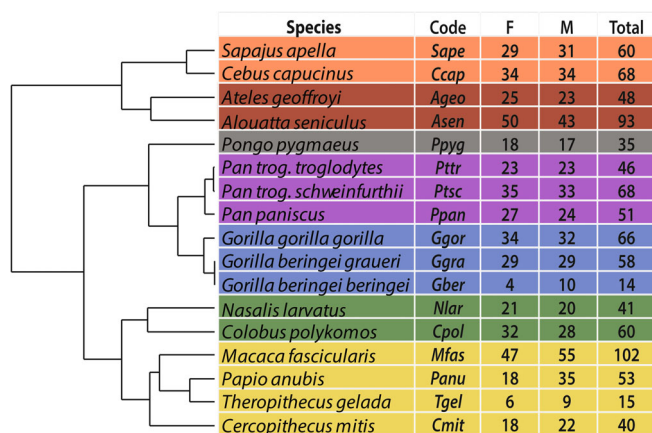


FIGURE 2 Samples employed in this analysis showing phylogenetic relationships (from 10KTrees), abbreviations used in the manuscript, and color coding by clade

primates, and our goal was instead to focus on variation in nonhuman primates rather than contrasting humans and other primate groups (which will instead be the focus of future work). All specimens were dentally adult (i.e., third molar erupted and in occlusion), though for a small number we noted that the third molars and/or canines were still in the process of eruption and may have been just shy of full occlusion. Approximately equal numbers of females and males were included in this sample. Specimens represent a range of adult ages and may include pathology and/or trauma to the cranium, dentition, and/or mandible. We purposefully included pathological individuals as one goal of this work is to examine the entire breadth of shape variation in the masticatory apparatus regardless of pathology or trauma. Analysis by our team (Mitchell et al., 2021) using our *Macaca fascicularis* sample reveals that the inclusion of pathological specimens does not radically alter the observed range of shape variation; in fact, purposeful exclusion of pathological specimens may artificially exclude portions of the range of variation more likely to accumulate skeletal lesions (e.g., old individuals, large males).

### 2.2 | Data collection

For each specimen, 3D models of the cranium and mandible were collected using either an HDI 120 blue-LED scanner or an HDI Advance (LMI Technologies) in the program FlexScan3D, or a Breuckmann SmartSCAN white light scanner in the program Optocat. Error analyses suggest that choice of scanner for data collection is likely to have little impact on gross shape analyses, especially those comparing differences in shape among species as we do here (e.g., Robinson & Terhune, 2017; Shearer et al., 2017). After scanning, models were imported into Geomagic Studio (3D Systems) and processed using the “Fill Holes” and “Mesh Doctor” functions, which enabled us to fill minor holes. Where the original scans were particularly large, models were decimated to reduce file size; however, in all cases decimated models still contained >500,000 triangles (average polygon count across all crania = 2,090,320, mandibles = 1,846,665). Cranial and mandibular models were imported into the program Landmark Editor (Wiley et al., 2005) and a series of fixed landmarks (83 on the cranium, 36 on the mandible) and semilandmarks (104 on the cranium, 74 on the mandible) were placed on each specimen by DRM (Figure 3; Tables S1 and S2). Landmarks were selected to reflect major features of the masticatory apparatus (e.g., tooth position, muscle attachments) as well as other major landmarks on the skull (e.g., bregma, foramen magnum position, orbit shape, and position).

The shape of the glenoid fossa was quantified separately from the cranium. For this, one of us (CET) clipped out the surface of the right glenoid in the program Geomagic Studio by identifying the line encircling the glenoid along which the joint capsule attaches (Figure 1). Specimens where the margin of the glenoid was unable to be reliably identified were excluded from analysis, and for those with postmortem damage (e.g., a broken zygomatic) to the right glenoid the left glenoid was instead clipped and reflected along the sagittal plane. Each of the clipped glenoids were then imported into Landmark Editor (Wiley et al., 2005) and a series of 16 control landmarks were equally distributed along the edges and in the center of the glenoid fossa. These control points, along with the .ply models for the glenoid, were imported into R (R Core Team, 2021) where the *geomorph* package (Adams & Otárola-Castillo, 2013; Adams et al., 2020) and the functions “build.template” and “digitalsurface” were used to place a total of 125 semilandmarks across the glenoid articular surface. To assess error related to the glenoid data collection protocol, we selected five specimens where the glenoid was clipped and landmarked four times per specimen and landmarked as described above. Error analysis found that repeated trials of the same individual consistently clustered together in morphospace

and were distinct from trials of other individuals (e.g., Robinson & Terhune, 2017), indicating that glenoid shape can be reliably captured using this method.

### 2.3 | Data analysis

Standard geometric morphometric protocols were used to analyze glenoid shape variation and its relationship to cranial and mandibular shape. First, each landmark dataset (glenoid, cranium, mandible) was subjected to generalized Procrustes analysis (GPA), where semilandmarks were allowed to slide to minimize bending energy. For the glenoid, semilandmarks included the 125 semilandmarks on the glenoid surface as well as 15 curve landmarks arranged around the margins of the glenoid (i.e., all control points mentioned above except the one in the center of the AE). GPAs were performed in the program R using the “gpagen” function in *geomorph*. Prior to analysis, we examined each dataset for outliers using the “plot.outliers” function; this allowed us to identify and correct any errors in the dataset (e.g., specimens that were landmarked incorrectly or that had sustained postmortem damage and needed to be removed from

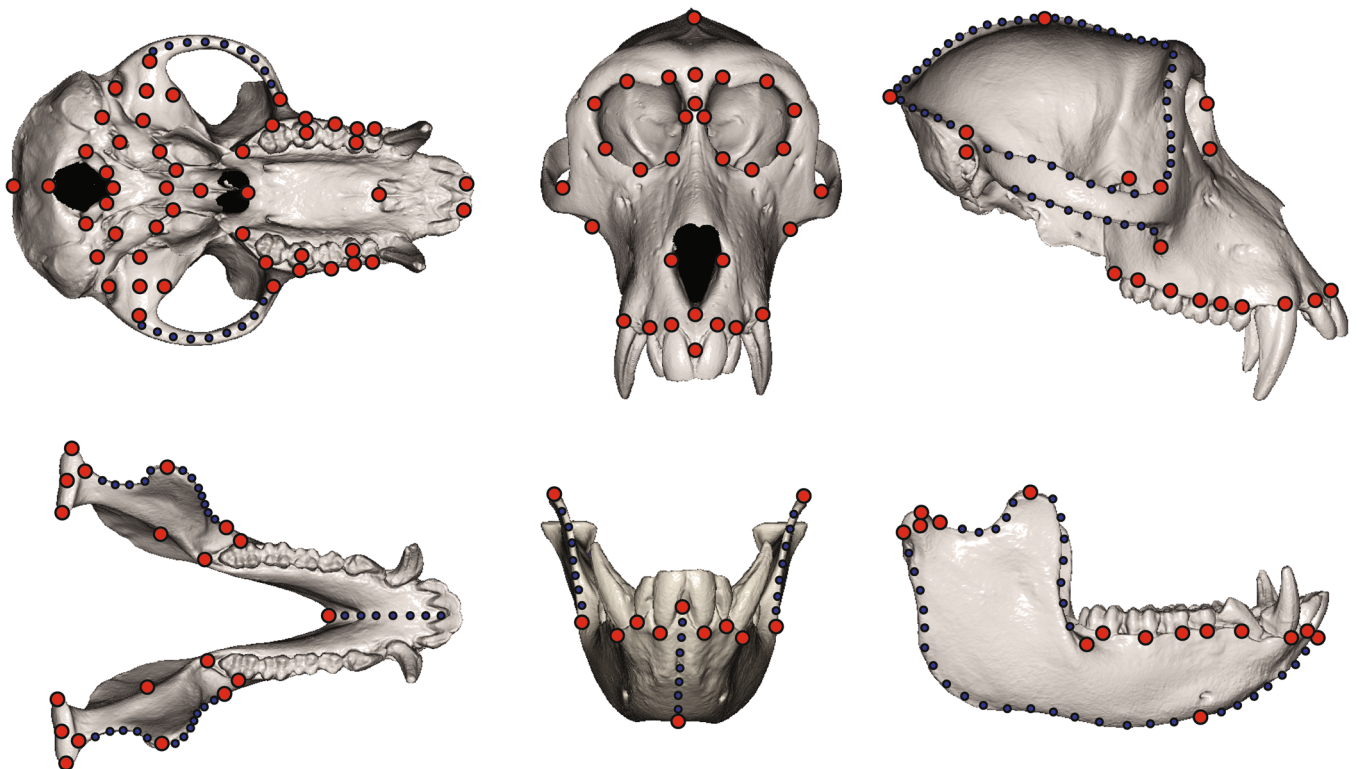


FIGURE 3 Numbered landmarks for the cranium and mandible as shown on a male *Macaca fascicularis* cranium (top) and mandible (bottom). Red = fixed landmarks, black = semi-sliding landmarks. See Tables S1 and S2 for corresponding descriptions

the analysis). Datasets were then exported from R as a TPS file for later use in the program MorphoJ (Klingenberg, 2011).

Variation in the entire dataset was first examined using a between group principal components analysis (bgPCA). This analysis was performed in MorphoJ, with additional visualizations conducted in SPSS (i.e., box plots of PC scores) and R (i.e., landmark configurations along bgPC axes). We regressed scores for the top three bgPC axes on the natural log of centroid size (lnCS) to examine the influence of size along each axis. We also performed a multivariate regression of the Procrustes residuals for the entire sample on lnCS (i.e., shape  $\sim$  ln [size]). To further investigate shape differences between species we calculated mean Procrustes distances between species in MorphoJ and used a permutation test (10,000 iterations) to calculate the significance of these differences. This allowed us to determine whether mean shapes between species/sexes were significantly different from one another; we further visualized and qualitatively described relevant mean shape differences between species.

Data were then averaged by species to perform a series of statistical analyses that allowed us to assess the significance of phylogeny and size in the sample. This included calculating the degree of phylogenetic signal (using the function “*physignal*” from *geomorph*) present (measured as a multivariate K-statistic; Adams, 2014) in the glenoid shape dataset and in glenoid centroid size as well as using the “*plotGMPhyloMorphoSpace*” function *geomorph* to overlay a phylogenetic tree on a PC plot of the species means of glenoid shape. We then used the “*procD.pgls*” function in *geomorph* to perform phylogenetic generalized least squares (PGLS) regressions of glenoid shape on glenoid CS, cranial CS, and mandible CS with 9999 iterations. For all phylogenetic analyses, we employed a consensus phylogeny of the 17 taxa included in the dataset downloaded from the website 10KTrees (Arnold et al., 2010; Figure 2).

Last, to evaluate how glenoid shape covaries with cranial and mandibular shape, we performed a series of two-block partial least squares (2BPLS) analyses using the “*two.b.pls*” function in *geomorph*. These analyses were conducted first on the raw shape data (glenoid vs. cranium, glenoid vs. mandible), and then using the regression residuals from PGLS regressions of each dataset on the natural log of cranial centroid size. This allowed us to adjust for the effects of both size and phylogeny in our 2BPLS analyses. For each 2BPLS model we generated rPLS values for the first singular axis, which describes the maximal covariation between the two blocks being analyzed (Rohlf & Corti, 2000). Statistical significance of the rPLS value

was assessed using a resampling procedure with 9999 iterations. For each model, we also report the multivariate effect size (Adams & Collyer, 2016, 2019) and the proportion of the total variance in size and shape that is expressed by that singular warp for that block of data (i.e., the percent of the total variance for a single block represented by that block’s first singular axis).

All of the analyses described above were performed for the entire sample and then again for females and males separately. We primarily present results (and especially visualizations) where the entire dataset is pooled but identify places where results diverge by sex. For all analyses alpha was set at 0.05.

### 3 | RESULTS

#### 3.1 | Between-Group PCA

In the bgPC plot of all individuals from both sexes (Figures 4 and 5), there is clearly variation related to clade, but there is also considerable within-group variation. bgPC1 explains 32.46% of the shape variation in the sample and is associated with the length and width of the glenoid surface as well as the size of the PGP and EGP. This axis largely separates the apes from both the cercopithecoid and platyrrhine taxa. On the negative end of this axis, the apes display relatively mediolaterally (ML) wide and anteroposteriorly (AP) short glenoid surfaces with small PGPs and large EGPs. Conversely, taxa falling more positively on this axis have anteroposteriorly long glenoids that are largely flat (i.e., less projecting processes and less raised AE) except for the large inferiorly projecting PGP.

Between group PC2 (Figures 4 and 5) represents 13.93% of the sample variation; shape variation along this axis is primarily associated with PGP and EGP size. This is similar to bgPC1 except in the combination of these features; negatively situated taxa have both a large EGP and large PGP, whereas positively situated taxa have small EGPs and PGP. This axis does not separate taxa as clearly as bgPC1, but generally platyrrhines and the gorillas tend to fall more negatively (i.e., large processes) while the cercopithecoids, orangutans, and chimps/bonobos fall more positively and tend to have flatter glenoids with small processes.

Between group PC3 (Figures 4 and 5), representing 10.8% of the sample variation, is slightly more difficult to interpret. This axis also represents aspects of PGP and EGP size but is associated with the ML and AP contours of the joint. Negatively positioned specimens

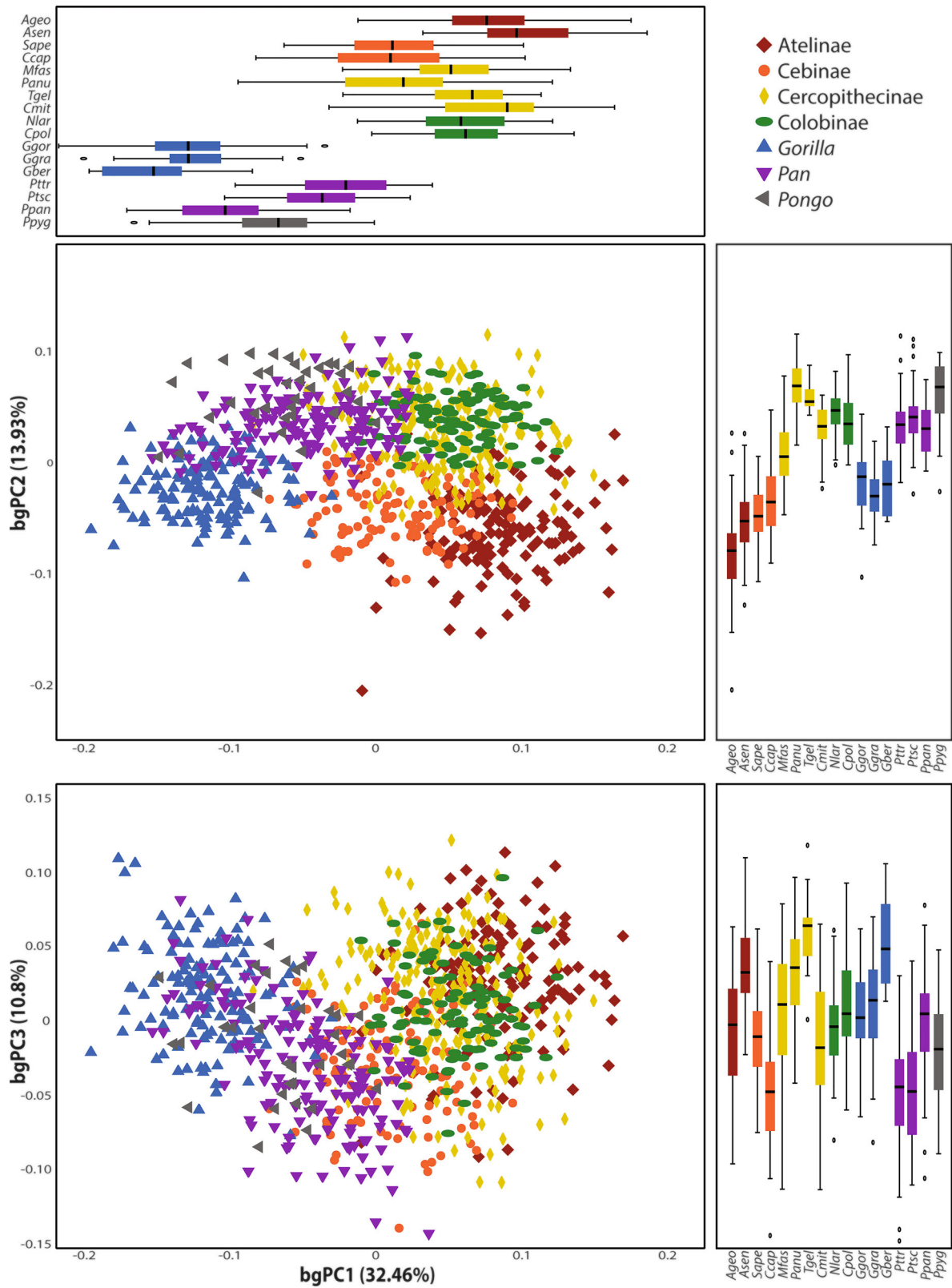


**FIGURE 4** Between-group principal component (bgPC) plots showing glenoid shape variation in morphospace and the distributions of species and clades on bgPCs1-3. Corresponding box plots show distributions of species on individual PC axes

have a relatively flat joint that curves gently inferiorly toward the EGP (i.e., is both ML and AP concave); these specimens also have a small PGP. In contrast,

more positively situated specimens/taxa have a larger PGP, a raised lateral aspect of the joint (near the articular tubercle) with a slight dip toward the AE,

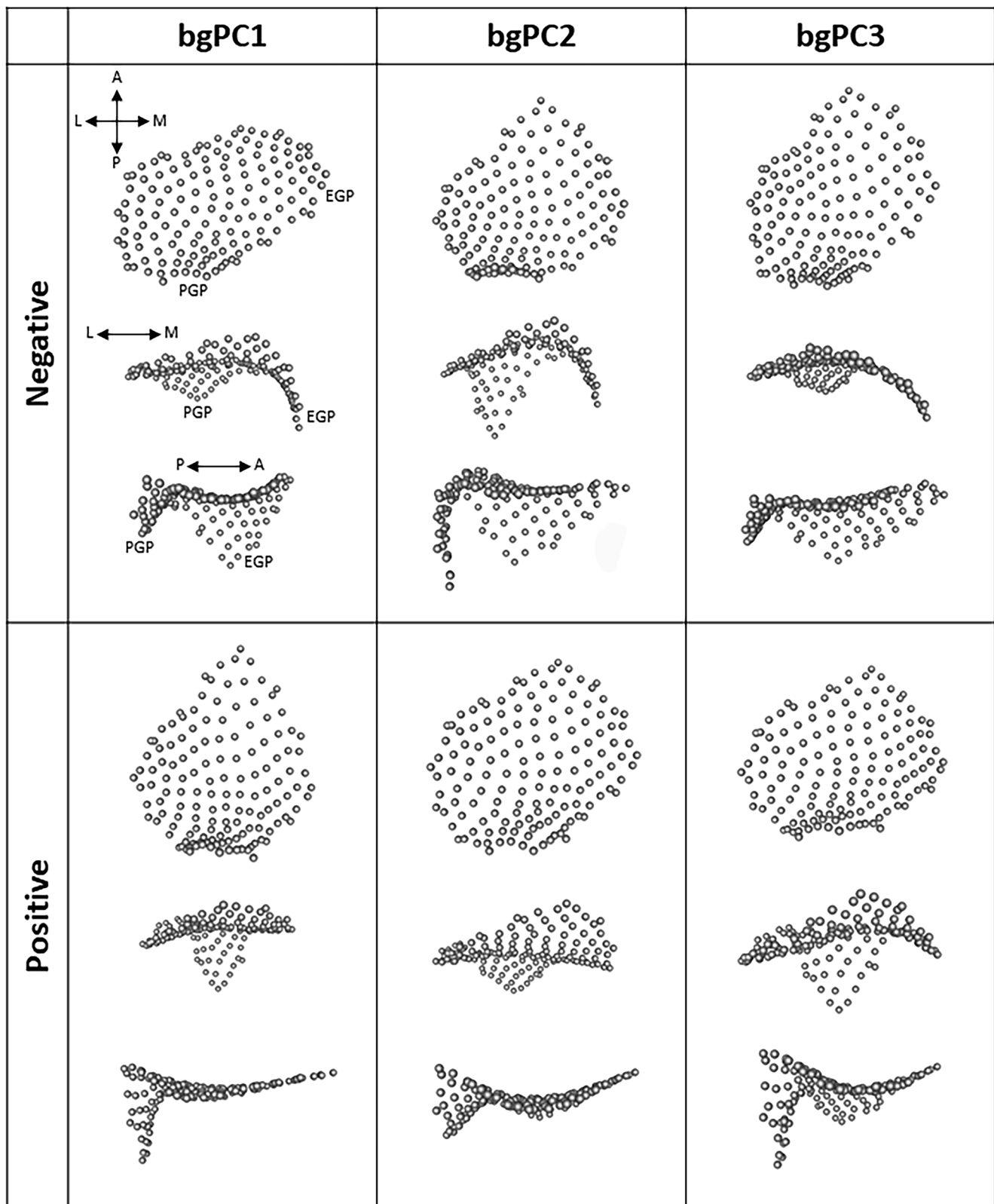


**FIGURE 5** Point clouds illustrating shape variation along between-group principal component axes 1–3 for the glenoid. For each set of visualizations (i.e., positive vs. negative) the top row = inferior view, middle row = anterior view, bottom row = lateral view. Directional arrows show orientation of glenoids (all of which are right joint surfaces); A, anterior, P, posterior, M, medial, L, lateral. EGP, entoglenoid process; PGP, postglenoid process

TABLE 1 Matrix of Procrustes distances among species means (sexes pooled)

	Ageo	Asen	Ccap	Cmit	Cpol	Gber	Ggor	Ggra	Mfas	Nlar	Panu	Ppan	Ppyg	Ptsc	Pttr	Sape
<i>Asen</i>	0.098															
<i>Ccap</i>	0.113	0.154														
<i>Cmit</i>	0.146	0.132	0.122													
<i>Cpol</i>	0.138	0.134	0.112	0.070												
<i>Gber</i>	0.234	0.246	0.190	0.237	0.214											
<i>Ggor</i>	0.208	0.229	0.146	0.204	0.187	0.072										
<i>Ggra</i>	0.203	0.221	0.149	0.201	0.185	0.070	0.052									
<i>Mfas</i>	0.121	0.118	0.096	0.066	0.068	0.204	0.173	0.168								
<i>Nlar</i>	0.153	0.144	0.112	0.063	0.049	0.217	0.187	0.188	0.071							
<i>Panu</i>	0.172	0.162	0.143	0.110	0.093	0.187	0.170	0.174	0.101	0.092						
<i>Ppan</i>	0.205	0.218	0.155	0.198	0.174	0.115	0.104	0.103	0.164	0.174	0.142					
<i>Ppyg</i>	0.208	0.217	0.144	0.165	0.150	0.152	0.115	0.132	0.147	0.151	0.120	0.098				
<i>Ptsc</i>	0.168	0.186	0.114	0.138	0.127	0.165	0.134	0.138	0.124	0.125	0.112	0.095	0.099			
<i>Pttr</i>	0.163	0.175	0.112	0.133	0.124	0.174	0.141	0.146	0.118	0.121	0.117	0.105	0.109	0.029		
<i>Sape</i>	0.107	0.137	0.060	0.126	0.119	0.180	0.145	0.143	0.092	0.119	0.137	0.152	0.152	0.132	0.130	
<i>Tgel</i>	0.163	0.145	0.159	0.127	0.091	0.220	0.205	0.208	0.104	0.101	0.081	0.175	0.164	0.152	0.149	0.147

Note: *p*-Values for all distances are  $p < 0.0001$  except between *Pan troglodytes troglodytes* and *Pan troglodytes schweinfurthii* ( $p = 0.027$ ). Species abbreviations are provided in Figure 2.

the contour of which moves more medially, and then a slight medial lip of the joint (i.e., small EGP). These taxa also tend to have a preglenoid plane that is inflected more superiorly. In other words, these taxa

have a more raised “bar-like” AE (the AP curvature of the joint is more convex). This axis does not clearly separate taxa by clade and instead likely represents intraspecific variation.

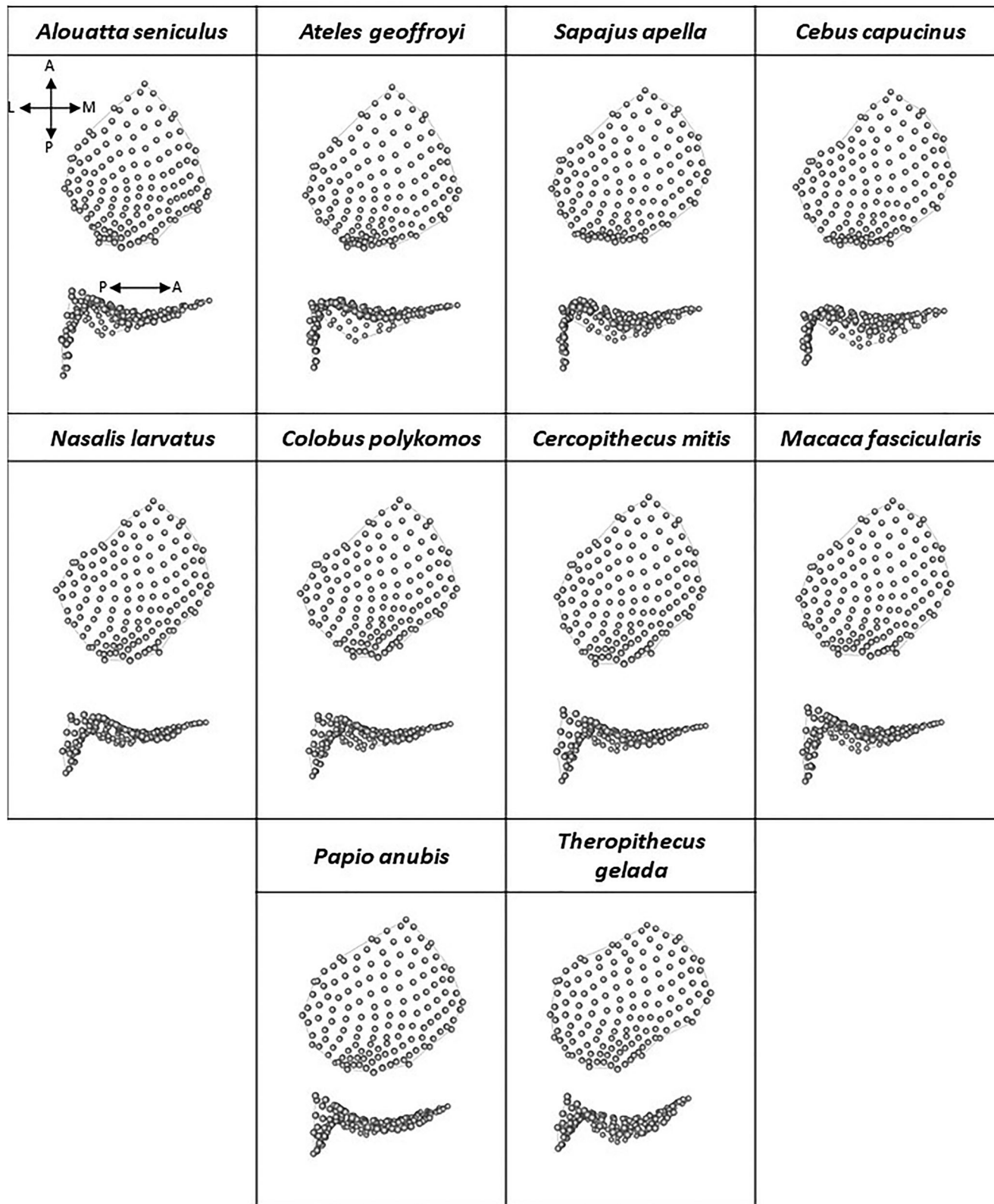


FIGURE 6 Point clouds illustrating mean platyrrhine and cercopithecoid species shapes for the glenoid. For each species, the top = inferior view, bottom = lateral view. Refer to Figures 1 and 5 for key to landmarks and orientation

All three of these axes, and indeed shape variation across the entire sample generally, are strongly related to glenoid centroid size. A multivariate regression of the glenoid shape for all individuals on glenoid lnCS returned an  $r^2 = 0.15$  with a corresponding  $p$ -value of  $<0.0001$ . Regression of individual bgPC scores against the natural log of glenoid CS also found a significant relationship between the top three bgPC axes and size (bgPC1:  $r^2 = 0.498$ ,  $p < 0.0001$ ; bgPC2:  $r^2 = 0.077$ ,  $p < 0.0001$ ; bgPC3:  $r^2 = 0.009$ ,  $p = 0.004$ ). However,  $r^2$  values for bgPCs 2 and 3 are very small and, therefore, size does not explain much of the shape variation observed.

Results when males and females are examined separately follow the same pattern described when sexes are pooled (Table S3).

### 3.2 | Shape differences among species

Procrustes distances among species means (where sexes were pooled) reveal significant differences in glenoid shape among all taxa examined (Table 1;  $p < 0.0001$ , except between *Pan troglodytes troglodytes* and *Pan troglodytes schweinfurthii*, where  $p = 0.027$ ). When sexes are examined

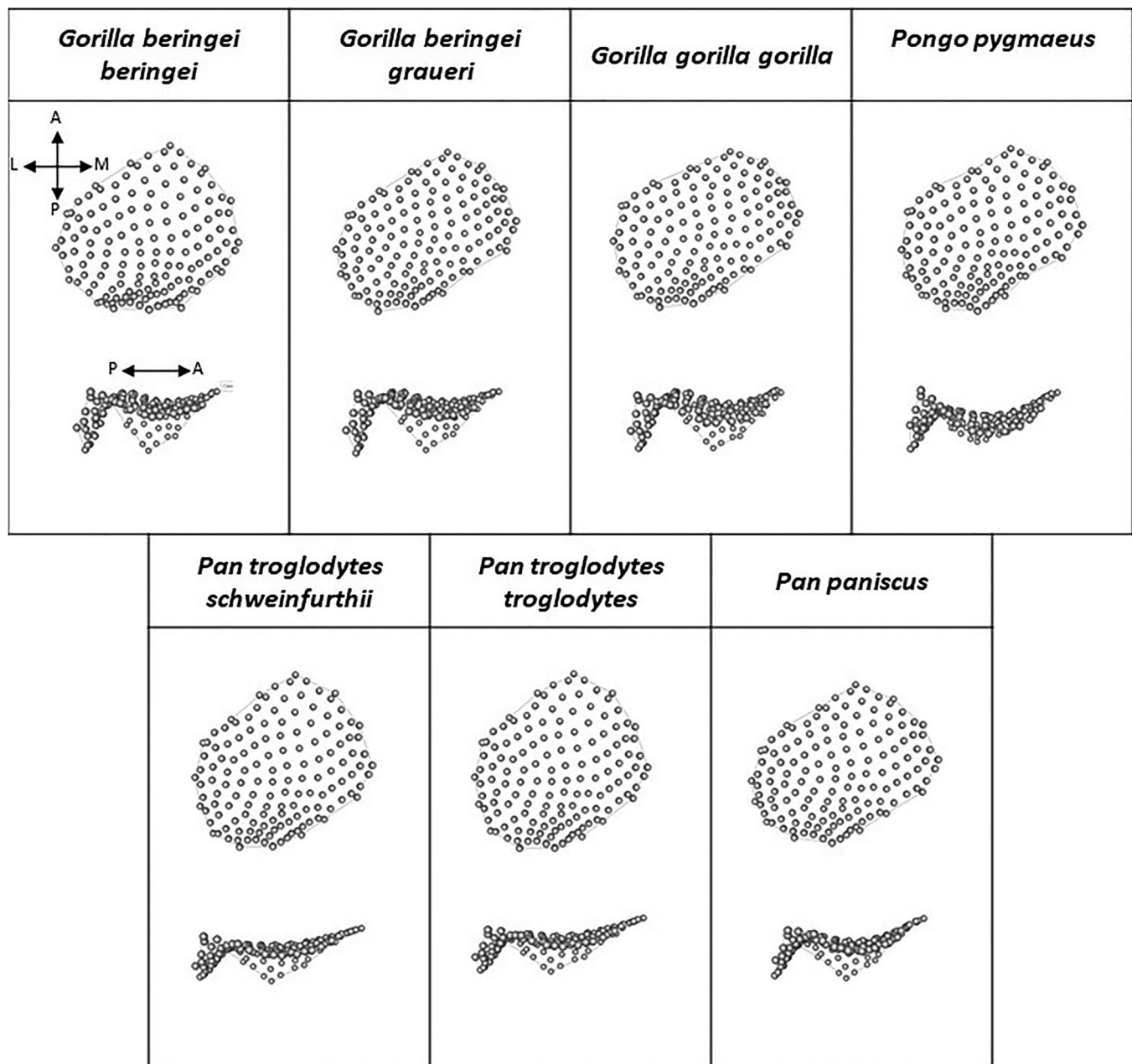


FIGURE 7 Point clouds illustrating mean great ape species shapes for the glenoid. For each species, the top = inferior view, bottom = lateral view. Refer to Figures 1 and 5 for key to landmarks and orientation

separately (Table S4), females show significant differences between all taxon pairs, and males follow the same pattern described when sexes are pooled (i.e., all pairs are significantly different except *Pan* subspecies [ $p = 0.26$ ]).

These differences in shape are manifested in a variety of ways (Figures 6 and 7). As described above, features that tend to vary among species are the length/width of the glenoid surface, the size of the PGP and EGP, the concavity of the joint, and the overall topography of the joint. Importantly, these features can appear in a variety of different combinations in different species, and there is substantial intraspecific variation such that there is considerable overlap in shape between species, especially those that are more closely related. In general, the platyrrhines (*A. seniculus*, *A. Geoffroyi*, *C. capucinus*, and *S. apella*; Figure 6) tend to have very similar glenoid shapes, all of which are concave both ML and AP with a medial joint aspect that slopes gradually inferiorly to form a slight EGP. In *A. seniculus* and *A. Geoffroyi*, the joint is slightly AP longer and the PGP is larger than in *C. capucinus* and *S. apella*, with *A. seniculus* having the largest, most inferiorly projecting PGP of all platyrrhine and catarrhine taxa examined.

The shape of the platyrrhine and cercopithecoid glenoid (Figure 6) is roughly similar, though the cercopithecoids tend to show a flatter overall glenoid surface with considerably less ML and AP concavity to the joint and relatively smaller EGPs than in platyrrhines. The PGP is moderately sized, though this feature varies across taxa. Most taxa also display a more classic “bar-like” AE (see Figure 1) running ML and with a distinct mandibular fossa between the eminence and the PGP.

Glenoid shape in *Gorilla*, *Pongo*, and *Pan* (Figure 7) is markedly different from that of the platyrrhines and cercopithecoids, and all three of these genera tend to have morphologies that are distinct from the other two. As in the cercopithecoids (but in contrast to the platyrrhines) the apes do have a clear “bar-like” AE (i.e., AP convexity), but all apes have considerably more topographic relief to their joints than is found in the cercopithecoids.

In *Pan*, the glenoid overall tends to be very flat and is slightly elongated AP. Both the EGP and PGP are relatively small, and the EGP does form a clear medial border to the joint (as in *Gorilla* but contra *Pongo*). Notably, the shape of the glenoid in *Pan paniscus* is slightly more similar to that of *Gorilla* (AP shorter, increased AP convexity, slightly larger PGP) than to the two subspecies of *Pan troglodytes* examined. *Pongo* exhibits a glenoid that is strongly convex AP, and intermediate in AP length between *Gorilla* and *Pan*. The medial aspect of the joint slopes gently to form a small EGP. All three *Gorilla* taxa examined share a distinctive joint morphology, where the articular surface is AP short and ML wide, the PGP is

slightly enlarged, and the EGP curves sharply inferior from the AE to form a clear medial wall to the joint.

Some taxa do exhibit significant differences in glenoid shape between sexes within species (Table S4). This includes *A. seniculus* ( $p < 0.0001$ ), *C. polykomos* ( $p = 0.0227$ ), *G. gorilla gorilla* ( $p = 0.003$ ), *G. beringei graueri* ( $p = 0.0021$ ), *M. fascicularis* ( $p < 0.0001$ ), *N. larvatus* ( $p = 0.0161$ ), *P. anubis* ( $p = 0.0018$ ), and *T. gelada* ( $p = 0.0424$ ). Morphological differences between sexes within species are subtle and will be described in separate, taxon-specific, publications.

### 3.3 | Phylogeny and size

As expected from the shape variation described above, glenoid shape is strongly patterned in relation to phylogeny (Figure 8). This is true regardless of whether sexes are pooled ( $K = 0.121$ ,  $p = 0.007$ ) or examined separately (females:  $K = 0.085$ ,  $p = 0.035$ ; males:  $K = 0.113$ ,  $p = 0.006$ ). Glenoid size also exhibits a significant phylogenetic signal (pooled:  $K = 0.536$ ,  $p = 0.021$ , females:  $K = 1.412$ ,  $p = 0.017$ , males:  $K = 1.092$ ,  $p = 0.001$ ).

PGLS regressions of glenoid shape on size (Table 2) revealed a significant relationship between glenoid shape and glenoid centroid size when the data were pooled ( $r^2 = 0.50$ ,  $p = 0.003$ ) and for females ( $r^2 = 0.62$ ,  $p = 0.002$ ) separately, but not males ( $r^2 = 0.15$ ,  $p = 0.096$ ). When glenoid shape was regressed on cranial centroid size the relationship was significant when sexes were pooled ( $r^2 = 0.42$ ,  $p = 0.007$ ), but not when sexes were examined separately (females:  $r^2 = 0.15$ ,  $p = 0.11$ , males:  $r^2 = 0.12$ ,  $p = 0.16$ ). Lastly, when glenoid shape was regressed on mandibular centroid size, there was a

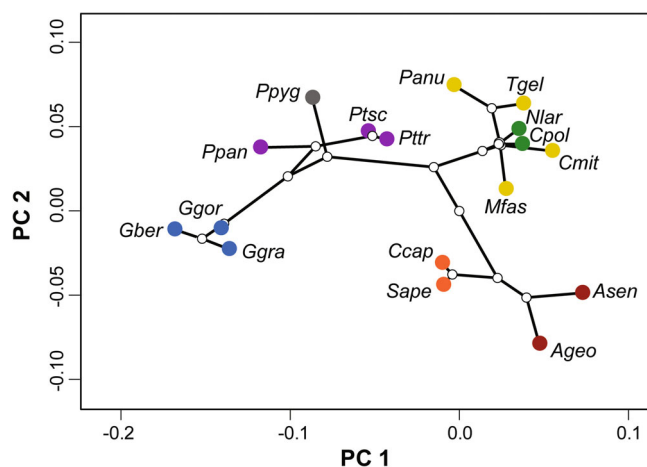


FIGURE 8 PC plot of species means (sexes pooled) overlaid with the phylogenetic tree shown in Figure 2. See Figure 2 for abbreviations

significant relationship when the samples were pooled ( $r^2 = 0.30$ ,  $p = 0.032$ ) and for females separately ( $r^2 = 0.28$ ,  $p = 0.038$ ), but not males ( $r^2 = 0.08$ ,  $p = 0.25$ ).

Shape variation related to glenoid centroid size (Figure 9) largely mirrors the variation described above

for bgPC1. Smaller species tend to have flatter joints with larger PGPs and joint surfaces that are more anteroposteriorly elongated. Larger species tend to have more AP compressed and ML wider joints with smaller PGPs but considerably larger EGPs.

**TABLE 2** Phylogenetic generalized least squares regression results of glenoid shape (dependent variable) on three measures of size (independent variable): Glenoid centroid size (glenoid CS), cranial centroid size (cranial CS), and mandible centroid size (mand CS)

Glenoid shape vs.	Sexes combined		Females only		Males only	
	$r^2$	$p$ -Value	$r^2$	$p$ -Value	$r^2$	$p$ -Value
Glenoid CS (PGLS)	0.50	0.003	0.62	0.002	0.15	0.096
Cranial CS (PGLS)	0.42	0.007	0.15	0.11	0.12	0.16
Mandible CS (PGLS)	0.30	0.032	0.28	0.038	0.08	0.25

Note: All size variables were log transformed for analysis. Values in gray are statistically significant ( $p < 0.05$ ).

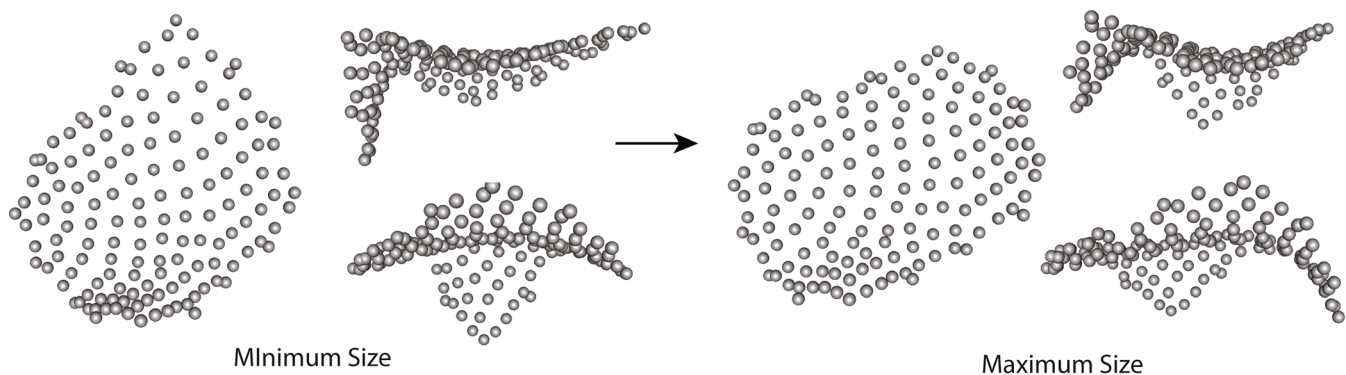
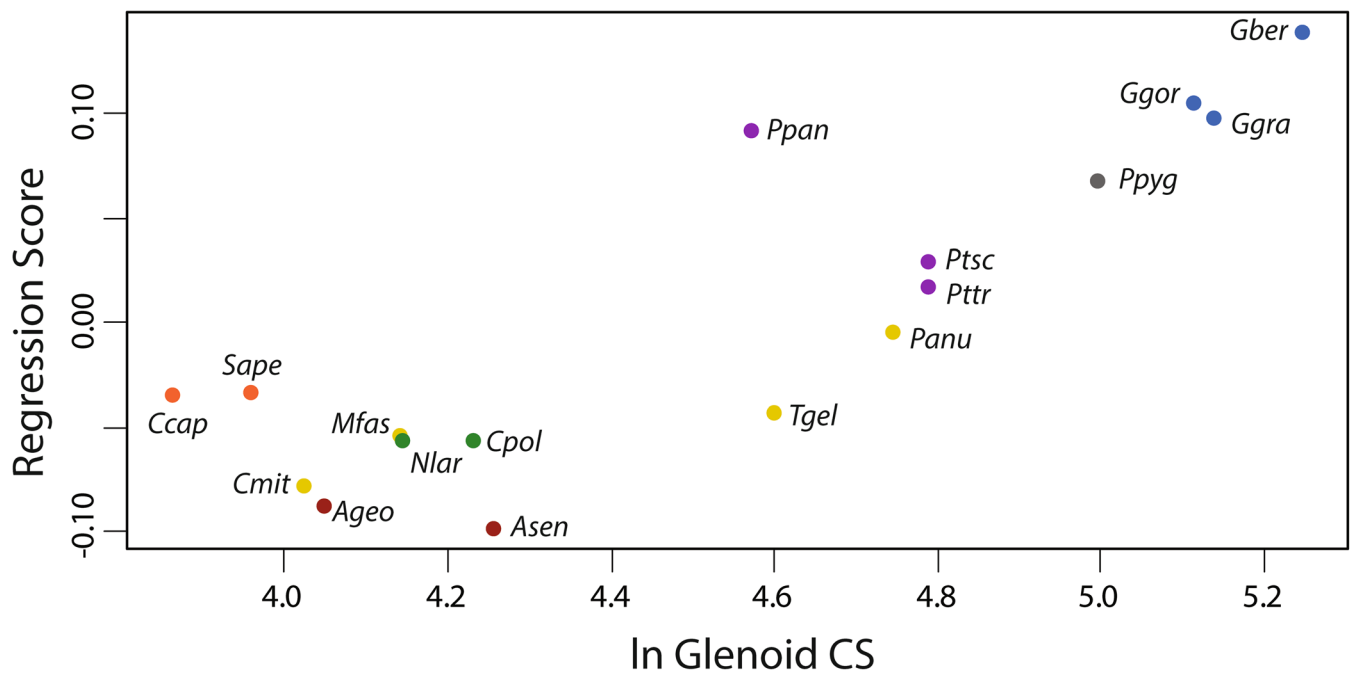


**FIGURE 9** Multivariate regression of the glenoid fossa configuration on the natural log of glenoid centroid size. Corresponding point clouds illustrate shape variation for small (minimum) versus large (maximum) species

TABLE 3 Results of the two-block partial least squares (2BPLS) analyses

	Sexes combined			Females only			Males only					
	%B1/%B2	rPLS1	p-Value	Effect	%B1/%B2	rPLS1	p-Value	Effect	%B1/%B2	rPLS1	p-Value	Effect
No adjustment for size or phylogeny												
Glenoid (B1) vs. cranium (B2)	44.3/30.7	0.79	0.011	2.35	45.6/35.0	0.77	0.019	2.16	42.8/25.5	0.83	0.0045	2.60
Glenoid (B1) vs. mandible (B2)	48.5/21.4	0.87	0.0009	3.01	50.1/25.0	0.87	0.0007	3.00	45.8/18.9	0.86	0.0007	2.95
Adjusted for size (cranCS) and phylogeny												
Glenoid (B1) vs. cranium (B2)	78.8/67.4	0.98	0.0001	5.39	76.8/55.3	0.98	0.0001	5.08	64.1/57.3	0.93	0.0001	4.55
Glenoid (B1) vs. mandible (B2)	78.8/76.1	0.98	0.0001	5.60	76.8/76.3	0.98	0.0001	5.44	63.8/57.4	0.93	0.0001	4.71

Note: Results include analyses of the raw data (i.e., no adjustment for size or phylogeny), and where phylogeny is incorporated into the model as well as size (cranial centroid size, cranCS). %B1/%B2 indicates the proportion of the total variance in size and shape that is expressed by the first singular warp for Block 1 (B1, glenoid fossa) and Block 2 (B2, either the cranium or mandible). rPLS1 represents the correlation between scores of projected values on the first singular axis for B1 and B2, and effect is the multivariate effect size of the given model.

### 3.4 | Covariation

The 2BPLS analyses revealed significant ( $p < 0.05$ ) covariance between glenoid shape and cranial/mandibular shape both before and after adjustment for size and phylogenetic covariation in the sample (Table 3; Figure 10).

In general, glenoid and cranial shape covary (Table 4; Video S1) such that, in species where the glenoid is flatter and more AP elongated (as in smaller individuals) the face tends to be smaller relative to the neurocranium, the temporal lines are set farther apart, the zygomatic arch is more gracile, palate is shorter and positioned roughly at the same level as the glenoid fossa, and the TMJ is positioned more posteriorly and laterally. In contrast, species with AP short, ML wide joints with more topography have larger faces relative to the neurocranium, temporal lines that converge more toward the midline (especially posteriorly), a deep (SI) zygomatic arch with more anteriorly positioned zygomatic root, a longer (AP) palate that is positioned well below the level of the glenoid fossa (i.e., TMJ height superior to the occlusal plane is increased), and a joint that is positioned more anteriorly and medially on the cranial base.

In the mandible (Table 4; Video S2), flatter, more AP elongated glenoids are found in species that have a supero-inferiorly deeper mandibular corpus at m2-m3, a more acute gonial angle that is slightly inverted, a narrower mandibular arch at the premolars/canines, and a ML narrow mandibular condyle, among other characteristics. Conversely, species with AP short and ML wide joints with more topographic relief tend to have a shallower corpus at m2-m3, a more obtuse gonial angle that is inverted and a condylar process that is more laterally positioned (i.e., the entire ramus is twisted such that the inferior margin is inverted and the superior margin is everted), a wider mandibular arch at the premolars/canines, and a ML wide condyle.

## 4 | DISCUSSION

The TMJ is the direct interface between the mandible and cranium and is therefore crucial for determining joint range of motion and transmission of joint reaction forces. However, only a handful of analyses have described shape variation in this structure, and even fewer have examined direct links between TMJ shape and the shape of the cranium and mandible. There were two goals of the present study: (1) assess shape variation in the glenoid fossa of anthropoid taxa and link this shape variation to phylogeny and body and/or cranial size, and (2) examine how glenoid fossa shape covaries

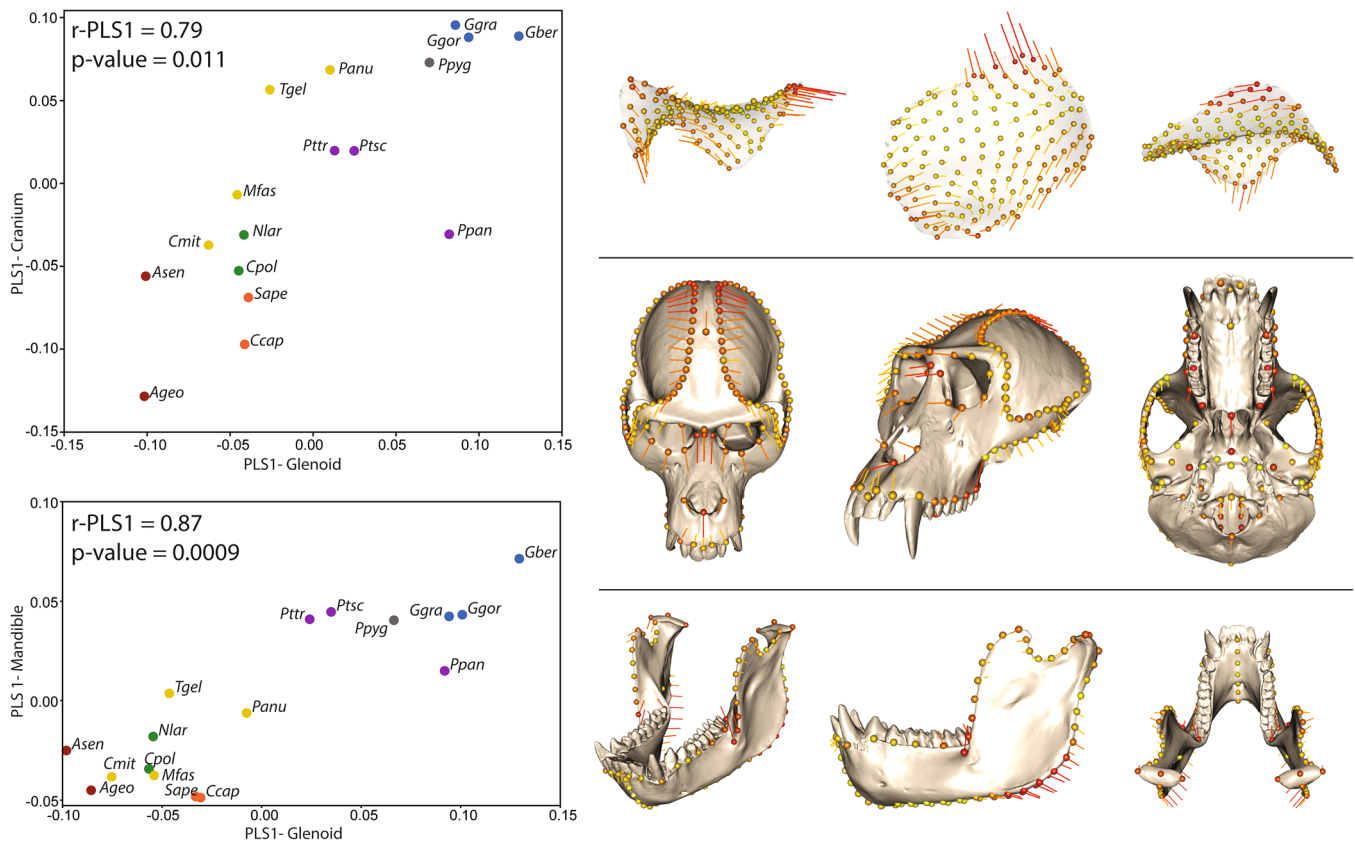


**FIGURE 10** Left: Bivariate plot of the partial least squares scores for the first singular vectors (PLS1) of the glenoid versus cranium (top) and mandible (bottom). Data shown are for both sexes pooled with no adjustment for size or phylogeny. Refer to Table 3 for rPLS values,  $p$ -values, and effect sizes. Right: Warped surface models and corresponding landmarks for the glenoid fossa (top), cranium (middle), and mandible (bottom). Meshes and landmarks shown correspond to positive ends of the relevant axes. Lines projecting from the landmarks show changes in shape from the negative ends of the axes to the shape shown; longer lines indicate more shape change. Redder colors indicate landmarks where more shape change occurs, whereas lighter colors indicate less shape change. Refer to Videos S1 and S2 for illustrations of these shape changes. Note that for the cranium, the average configuration was that of a male *Nasalis larvatus*, thus the large canines (the shape of which is not captured by our landmark dataset)

with cranial and mandibular shape across anthropoids. The data here confirm that there is considerable glenoid shape variation both across and within species, that major aspects of this shape variation are patterned in relation to phylogenetic relationships and body size, and that some species show sexual dimorphism of the glenoid. Further, we demonstrate that shape variation in the glenoid, cranium, and mandible show very high levels of covariation, as would be expected given that these anatomical units must function together during both masticatory and non-masticatory behaviors.

#### 4.1 | Shape variation among species

That there is variation in glenoid shape across primates is visible even in the absence of the quantitative analyses presented here; this variation has been noted and examined previously by a variety of authors (e.g., Ashton &

Zuckerman, 1954; Bouvier, 1986a, 1986b; Smith et al., 1983; Taylor, 2005; Terhune, 2011a, 2011b, 2013a, 2013b; Vinyard et al., 2003; Wall, 1997, 1999). As we further demonstrate, clear (though sometimes subtle) differences exist in mean glenoid shape among species and clades across primates. Platyrrhines and cercopithecoids share similar glenoid shapes, where the glenoid surface is typically AP elongated and there is a large PGP. However, cercopithecoids show an overall flatter glenoid surface with much less ML and AP concavity and smaller EGPs. Hominoid glenoid morphology tends to be the most distinct in that they have ML wider and AP shorter joints, a much more pronounced EGP that forms a clear medial border to the joint, and a more raised AE.

It is also clear from these results that a large portion of this shape variation is related to size variation among species and clades. Again, this has been noted before for the TMJ (e.g., Smith et al., 1983; Terhune, 2017), but never examined systematically across such a large sample

TABLE 4 Descriptions of the shape variation associated with the 2B-PLS analysis

	Negative	Positive
Glenoid	<ul style="list-style-type: none"> <li>• AP long joint</li> <li>• Flat joint contours</li> <li>• Large PGP</li> <li>• Small EGP</li> <li>• Flat preglenoid plane</li> <li>• Joint more elongated along sagittal axis</li> </ul>	<ul style="list-style-type: none"> <li>• AP short, ML wide joint</li> <li>• More joint topography</li> <li>• Small PGP</li> <li>• Large EGP</li> <li>• Preglenoid plane angled superiorly (forming more distinct articular eminence)</li> <li>• Joint elongated along axis running more postero lateral to antero medial</li> </ul>
Cranium	<ul style="list-style-type: none"> <li>• Small face relative to neurocranium</li> <li>• Temporal lines set far apart, especially posteriorly</li> <li>• Shallow/gracile zygomatic arch</li> <li>• Maxillary arch more open posteriorly</li> <li>• Shorter palate/face</li> <li>• Palate positioned close to same level as zygomatic arches and glenoid (TMJ is closer to occlusal plane)</li> <li>• Long basioccipital</li> <li>• Joint positioned more posteriorly and medial aspect of joint does not project as far medially toward midline</li> </ul>	<ul style="list-style-type: none"> <li>• Large face relative to neurocranium</li> <li>• Temporal lines more likely to converge, especially posteriorly</li> <li>• Deep zygomatic arch with more anteriorly positioned zygomatic root</li> <li>• Maxillary arch more pinched posteriorly</li> <li>• Longer palate/face</li> <li>• Palate positioned considerably more inferiorly, well below level of TMJ/zygomatic arches (TMJ is well above occlusal plane)</li> <li>• Short basioccipital</li> <li>• Joint positioned slightly more anteriorly, and medial aspect of joint positioned more antero-medial</li> </ul>
Mandible	<ul style="list-style-type: none"> <li>• Slightly more inclined mandibular symphysis</li> <li>• Supero-inferiorly deeper corpus at m2-m3</li> <li>• More acute gonial angle that is more inverted</li> <li>• Narrower mandibular arch at premolar/canines</li> <li>• Corpus more upright</li> <li>• Condyle ML narrower</li> <li>• Coronoid process more symmetric and directed superiorly</li> <li>• Long axis of condyle angled more posteromedial/anterolateral</li> <li>• Root of ramus closer to alveolar margin</li> </ul>	<ul style="list-style-type: none"> <li>• Slightly more vertical mandibular symphysis</li> <li>• Shallower corpus at m2-m3</li> <li>• More obtuse gonial angle that is everted</li> <li>• Wider mandibular arch at premolars/canines</li> <li>• Corpus angled more infero/laterally to supero/medially (whole corpus including gonial angle is more everted with condyle more inverted)</li> <li>• Condyle ML wider</li> <li>• Coronoid process slightly more angled posteriorly</li> <li>• Long axis of condyle oriented more in coronal plane</li> <li>• Root of ramus begins more inferiorly</li> </ul>

Note: All shapes described are for the first singular vector (see Figure 10).

Abbreviations: AP, anteroposterior; EGP, entoglenoid process; ML, mediolateral; PGP, postglenoid process; TMJ, temporomandibular joint.

using detailed shape data. Both multivariate regressions of glenoid shape and individual PC axes on size (glenoid and cranial) returned significant relationships, though this signal varied slightly depending on whether the data were adjusted for phylogeny and whether the sexes were combined. One interesting result was the PGLS analyses of glenoid shape on glenoid centroid size, which found a significant relationship in females but not males. This result partly mirrors those of Terhune (2017), who found that

relationships between glenoid fossa shape (as represented by 12 fixed landmarks) and either mandible length or body mass were not consistent across taxonomic groups or sexes. However, in that analysis glenoid shape in males tended to show a stronger relationship to mandible length and/or body size than glenoid shape in females did, which is the opposite of the result here. Reasons for this discrepancy are unclear but could be related to sample composition and/or landmarks. One possible explanation for the

results found here is that glenoid morphology in male primates is more constrained because of their relatively larger canine crown heights. Specifically, many anthropoid primates display considerable canine size dimorphism (Plavcan 1990, 2001), and these large canine crown sizes have been closely linked to jaw gape (Hylander, 2013). Further, jaw gape (relative to mandible length) tends to be larger in cercopithecoids than in hominoids and in males compared to females. Since jaw gape is at least partly determined by range of motion at the TMJ, it is possible that male primates in particular are more limited in the shape of their glenoid so that they can achieve these large gapes.

The allometric variation we observed in glenoid shape relative to glenoid and cranial size mirrored the differences described above among clades. In part, this is a function of overall body size differences between the clades examined, though some species with similar glenoid centroid sizes (e.g., *A. seniculus* vs. *C. polykomos* and *T. gelada* vs. *P. paniscus*) did show distinct differences in glenoid shape (Figure 9). Coupled with the analyses of phylogenetic signal in glenoid shape and size, it is therefore clear that there is also strong phylogenetic patterning in the dataset. This was also identified by Terhune (2017), but no other analyses to date have analyzed TMJ shape in a phylogenetic context. Of course, phylogeny and size as well as feeding behaviors are closely intertwined, making it difficult to tease apart the influences of all three of these factors.

#### 4.2 | Shape variation within species

Patterning of the variation in glenoid shape documented here is somewhat obscured by the considerable intraspecific variation present. As evidenced by the between group PC plots, many species overlap considerably in shape space in their glenoid morphology, and the ranges of variation within each species are often considerable. In addition to idiosyncratic variation, there are likely two major factors that contribute to this variation: sexual dimorphism and joint remodeling.

Though we did test for differences in glenoid shape between males and females in our sample, it was not a major focus of this study. However, we did identify that about half (8 out of 17) of taxa showed significant differences in mean glenoid shape between males and females. Not surprisingly, this included species where craniofacial sexual dimorphism is relatively pronounced, such as in *Alouatta*, *Gorilla*, and all but one (*Cercopithecus*) of the cercopithecoid species sampled. Though we did not go into detail on the morphological differences between sexes in each of these clades, previous research by

Terhune et al. (2015) has shown that male and female *Macaca fascicularis* show clear differences in condylar, mandibular, and soft tissue anatomy that is almost certainly related to selection for increased canine crown height in males. Additional analyses (Taylor et al., 2018) looking at muscle architecture and leverage across papioinins (*Macaca fascicularis*, *Macaca mulatta*, *Papio anubis*, *Cercocebus atys*) found the same pattern with regard to selection for increased jaw excursion in males relative to females. Given that differences in feeding behaviors between males and females within these species are not documented, these differences are almost certainly related to the well-documented canine display behaviors in these and other sexually dimorphic primates where there is strong male–male competition (e.g., Plavcan et al., 1995). These behaviors likely explain a large amount of the intraspecific variation in glenoid morphology found in this analysis; future analyses will focus on examining sexual dimorphism in glenoid shape in specific species.

Joint remodeling also likely contributes to the high levels of intraspecific variation observed here. A wide variety of histological, comparative, and clinical studies (e.g., Granados, 1979; Hinton, 1981; Jasinovicus et al., 2006; Kurita et al., 2000; Moffett et al., 1964; Richards, 1988; Yamada et al., 2004) have examined how the contours of the TMJ change in relation to dental function, with most agreeing that, at least in humans, the AE remodels extensively in relation to tooth wear and typically becomes flatter with age. Others agree that there is considerable variation in the shape of the TMJ both among and within human populations. For example, Osborn and Baragar (1992) looked at a sample of human condyles and found that condylar shape varied greatly and seemed to be at least partly correlated with modeled force distributions in the TMJ. Koppe et al. (2007) examined glenoid shape in 30 skulls from Iron Age and medieval populations from Lithuania and mixed Neolithic and Bronze age populations from the Central Elbe-Saale of Germany and found that glenoid shape varied significantly among the three populations and that all showed considerable fluctuating asymmetry (i.e., random deviations from symmetry). Hinton (1983) similarly found differences in joint size in different human populations that he linked to masticatory stresses (simply, increased masticatory stresses are related to larger joint sizes). He also suggested (Hinton, 1981) that AE depth varied in relation to dental wear, such that the eminence became shallower with increased molar wear (and by proxy, age); a result duplicated by Moffett et al. (1964). However, patterns of changes in the shape of the AE somewhat depended on the population being examined and whether wear was concentrated on the anterior versus posterior teeth. Last,

Hinton and Carlson (1979) found changes in TMJ size across the last 10,000 years of human evolution, observing a trend toward reducing TMJ size over time, likely as a function of decreased masticatory activity and increasing gracility linked to the shift from hunting and gathering to agriculture.

Thus, it's clear that there is considerable variation in TMJ form, and at least some of this variation is linked to functional demands of the masticatory apparatus and joint remodeling in relation to dental function and/or wear. What is less clear is how this translates to non-human primates, since no studies to date (with the exception of Terhune et al. [2015]) have investigated intraspecific variation in the glenoid in primates. In fact, to our knowledge, only one other study (Curth et al., 2017) has explicitly examined intraspecific variation in the TMJ, finding high levels of variation in the TMJ in domestic dogs relative to wolves, which they link to relaxed selection on masticatory function in dogs and the high levels of artificial selection for particular cranial shapes in this group. Dietary variation, dental function/wear, and the presence or absence of craniodental lesions or trauma are, therefore, almost certainly related to some of the intraspecific variation we observe in our primate sample here; this question is the subject of ongoing work by our research team.

### 4.3 | Covariation between glenoid, cranial, and mandibular shape

One trend in previous analyses of the masticatory apparatus is that different parts of this system tend to be analyzed separately from one another. This atomization of the masticatory apparatus into its constituent parts belies the fact that all of these parts must function in harmony in order to achieve adequate processing and/or mastication of food items as well as producing a particular gape or vocalization. As a result, one of the goals here was to examine covariation between the shapes of the cranium, mandible, and glenoid; ultimately these analyses will be extended to include aspects of dental occlusal morphology, wear, and craniofacial pathologies.

Only two analyses have specifically examined these patterns of covariation before. The first, by Terhune et al. (2015) looked at the relationships between the cranium, mandible, glenoid fossa, mandibular condyle, and the upper and lower molars in a sample of 10 platyrrhine species. This served as a pilot study for the larger analyses focusing on the glenoid that are presented here as well as future analyses planned by our research team. However, this research specifically examined covariation between the teeth vs. cranial or TMJ morphology (and found

strong patterns of covariance), but did not look at covariation between the glenoid and other aspects of cranial or mandibular shape.

Work by Curth et al. (2017) used geometric morphometrics to assess whether skull form predicts TMJ shape in wolves and dogs. As noted above, they found that TMJ shape is more diverse in dogs than wolves, and they also found a significant relationship between cranial and mandibular shapes and TMJ shape, though at least some of this variation is likely related to overall body size. Specifically, they found that dogs and wolves with more dolichocephalic (long, narrow) crania have more "robust" TMJs with wider and more cylindrical mandibular condyles and a glenoid fossa that has a strong PGP (retroarticular process) that is more projecting and curves around the mandibular condyle. Conversely, brachycephalic (broad, short) crania have more gracile features of the TMJ and condyle with a flat glenoid fossa and a small PGP. These results are broadly similar to those we identify here, where primates with smaller, less projecting faces tend to have flatter joints with smaller processes, while those with larger, more projecting faces and that are overall more robust tend to have TMJs that are AP shorter and ML wider with more topographic relief. These similarities in patterns between primates and carnivores are notable and may suggest underlying similarities in masticatory and TMJ function and/or similarities in patterns of bone growth and development (Curth et al., 2017). Further work is warranted to examine whether these patterns extend across a broader range of mammalian groups, and to assess the biomechanical correlates of these patterns.

### 4.4 | Biomechanical implications

Variation in masticatory shape is often difficult to assess because of the interplay between diet, body size, and phylogenetic patterns. As is apparent from this and many other works (e.g., Bouvier, 1986a, 1986b; Hylander, 1979; Ross & Iriarte-Diaz, 2014; Ross et al., 2012; Taylor et al., 2015; Vinyard, 2008; Vinyard et al., 2011), these three factors intertwine such that it can be difficult to look only at how shape variation may be related to diet and feeding behavior. Further, the relationships between feeding behavior and masticatory morphology are challenging to assess in the first place, since a myriad of hierarchically related and non-mutually exclusive behaviors and loading regimes likely affect craniofacial morphology (i.e., Ross et al., 2012). Ultimately, the primate masticatory apparatus almost certainly follows a many-to-one pattern (i.e., Wainwright et al., 2005), where multiple different morphologies are capable of achieving the same

performance goals in regard to jaw gape and force production/dissipation. This is particularly clear from prior studies (e.g., Ross et al., 2012; Vinyard et al., 2008) that have found that mandibular kinematics and masticatory muscle activation patterns vary considerably even within a single chew cycle and often idiosyncratically among individuals. This variability is most likely a result of variation in food bolus size, shape, and material properties throughout the chewing cycle, and is also likely related to inter-individual variation in the morphology of the muscles, TMJ, and teeth (Ross and Iriarte-Diaz, 2014). One additional source of this variation could also be fluctuating asymmetry across the cranium and/or mandible (e.g., Romero et al., 2022).

Our results here are consistent with these previous findings and suggest that perhaps relatively small levels of variation in range of motion and force distribution at the TMJ do not substantially impact masticatory function, at least within a particular primate species. This is also consistent with findings by Curth et al. (2017), which identified substantial variation in TMJ shape, even within small samples of a single dog breed. While Curth et al. (2017) suggest this variation may be a result of relaxed selection on the masticatory apparatus and perhaps increased modular independence of the TMJ in dogs as a result of domestication, in primates it is most plausible to link these high levels of variation to increased behavioral flexibility and feeding behaviors and diet. This could be a function of seasonal variation in food availability and/or the exploitation of fallback foods (e.g., Lambert and Rothman, 2015; Marshall et al., 2009).

While one of the major features of the data here is the considerable variation in glenoid shape we observe, there are also some patterns in the data that might be biomechanically informative. For example, the data here are consistent with previous work by Taylor (2005) and Terhune (2013a, 2013b) that looked at variation in TMJ dimensions in the great apes, and specifically found ML wider dimensions in taxa that eat more resistant diets (e.g., mountain gorillas and bonobos). Interestingly, bonobos tend toward being an outlier in many of our analyses, perhaps because they seem to combine relatively smaller glenoid and cranial sizes (in comparison to the other apes) with glenoid morphologies that are more consistent with larger bodied species such as gorillas. This morphological convergence is consistent with behavioral convergences in the consumption of resistant foods such as pith and terrestrial herbaceous vegetation in bonobos and gorillas (e.g., Malenky & Stiles, 1991; Malenky & Wrangham, 1994; Serckx et al., 2015; Tutin & Fernandez, 1993; Williamson et al., 1990). Conversely, though our sample for *Theropithecus* is small, this species tends to show a distinct glenoid morphology relative to other cercopithecoids, perhaps as a result of their unique

dietary niche of grammivory (i.e., Jarvey et al., 2018). One possible interpretation of the data presented here is that differences in glenoid and TMJ shape among species may be more clearly linked with patterns of occlusion as a function of dental morphology (e.g., cusp relief) and/or variation in patterns of muscle leverage (i.e., Ross & Iriarte-Diaz, 2014; Ross et al., 2012). In regard to leverage patterns, one important aspect of biomechanics to note is that changes in the position of the bite point relative to the joint may explain the covariation we observe between relatively longer faces and glenoids with increased robusticity and/or joint relief (i.e., larger processes). Specifically, more anteriorly positioned bite points (i.e., as would occur when the face is elongated) should result in higher joint reaction forces (i.e., Hylander, 1977, 2006; Mitchell, 2019), which must then be adequately dissipated by either soft or hard tissue structures at the joint. Future analyses will explore covariation between TMJ, craniofacial, and dental shape as well as relationships between the glenoid fossa and measures of masticatory performance and efficiency.

## 5 | CONCLUSIONS

We present the most comprehensive analysis of glenoid shape variation to date and the first analysis to examine covariation between glenoid shape and other aspects of craniofacial shape. Glenoid shape is patterned in relation to both size and phylogeny across our sample, and relatively high levels of intraspecific variation may reflect sexual dimorphism (at least in some species), pathologic processes and remodeling of the TMJ, and/or functional flexibility of the TMJ that is reflected in high levels of kinematic and muscle activity patterns in a single chew cycle within and between individuals. Further work is necessary to relate these patterns of shape variation to variation in dental morphology, rates of pathologic lesions, and masticatory performance across primates.

## ACKNOWLEDGMENTS

We thank all of the collections managers and researchers who enabled our access to materials used in this study: William Stanley, Lawrence Heaney, and Adam Ferguson (Field Museum of Natural History); Neil Duncan and Marisa Surovy (American Museum of Natural History); Lyman Jellema and Johannes Haile-Selassie (Cleveland Museum of Natural History); Brenda Baker (Arizona State University); Emmanuel Gilissen (Royal Museum for Central Africa); and Darin Lunde (Smithsonian National Museum of Natural History). We also thank students Christopher Carter and Logan Hearp for their work processing and organizing the 3D data. This research was

supported by funding from the National Science Foundation (BCS-1551766 to CET, BCS-1551669 to CAK, and BCS-1551722 to SBC) with additional funding was provided by Bernard Wood and The George Washington University to JM.

## CONFLICT OF INTEREST

The authors declare that they have no conflict of interest.

## AUTHOR CONTRIBUTIONS

**Claire E. Terhune:** Conceptualization (lead); data curation (equal); formal analysis (lead); investigation (lead); methodology (lead); project administration (equal); visualization (lead); writing – original draft (lead). **D. Rex Mitchell:** Conceptualization (supporting); data curation (equal); formal analysis (supporting); investigation (supporting); methodology (supporting); writing – review and editing (equal). **Siobhán B. Cooke:** Conceptualization (supporting); data curation (equal); project administration (equal); writing – original draft (supporting); writing – review and editing (equal). **Claire Kirchhoff:** Conceptualization (supporting); data curation (equal); project administration (equal); writing – original draft (supporting); writing – review and editing (equal). **Jason Massey:** Data curation (equal); resources (equal); writing – review and editing (equal).

## DATA AVAILABILITY STATEMENT

3D models used in this research are available on MorphoSource under the project name *Normal and pathological covariation in the masticatory apparatus of anthropoid primates*.

## ORCID

Claire E. Terhune  <https://orcid.org/0000-0002-5381-2497>

D. Rex Mitchell  <https://orcid.org/0000-0003-1495-4879>

Siobhán B. Cooke  <https://orcid.org/0000-0001-8265-6705>

Claire A. Kirchhoff  <https://orcid.org/0000-0002-9375-6282>

Jason S. Massey  <https://orcid.org/0000-0003-4681-6323>

## REFERENCES

- Adams, D., Collyer, M., Kaliontzopoulou, A., & Sherratt, E. (2020). Geomorph: Geometric morphometric analyses of 2D/3D landmark data. R package version 3.2, 1.
- Adams, D. C. (2014). A generalized K statistic for estimating phylogenetic signal from shape and other high-dimensional multivariate data. *Systematic Biology*, *63*, 685–697.
- Adams, D. C., & Collyer, M. L. (2016). On the comparison of the strength of morphological integration across morphometric datasets. *Evolution*, *70*, 2623–2631.
- Adams, D. C., & Collyer, M. L. (2019). Comparing the strength of modular signal, and evaluating alternative modular hypotheses, using covariance ratio effect sizes with morphometric data. *Evolution*, *73*, 2352–2367.
- Adams, D. C., & Otárola-Castillo, E. (2013). Geomorph: An R package for the collection and analysis of geometric morphometric shape data. *Methods in Ecology and Evolution*, *4*, 393–399.
- Arnold, C., Matthews, L. J., & Nunn, C. L. (2010). The 10KTrees website: A new online resource for primate phylogeny. *Evolutionary Anthropology*, *19*, 114–118.
- Ashton, E. H., & Zuckerman, S. (1954). The anatomy of the articular fossa (fossa mandibularis) in man and apes. *American Journal of Physical Anthropology*, *12*, 29–61.
- Baragar, F. A., & Osborn, J. W. (1984). A model relating patterns of human jaw movement to biomechanical constraints. *Journal of Biomechanics*, *17*, 757–767.
- Baragar, F. A., & Osborn, J. W. (1987). Efficiency as a predictor of human jaw design in the sagittal plane. *Journal of Biomechanics*, *20*, 447–457.
- Bennett, N. G. (1908). A contribution to the study of the movements of the mandible. *Proceedings of the Royal Society of Medicine*, *1*, 79–98.
- Bouvier, M. (1986a). Biomechanical scaling of mandibular dimensions in new-world monkeys. *International Journal of Primatology*, *7*, 551–567.
- Bouvier, M. (1986b). A biomechanical analysis of mandibular scaling in old-world monkeys. *American Journal of Physical Anthropology*, *69*, 473–482.
- Curth, S., Fischer, M. S., & Kupczik, K. (2017). Can skull form predict the shape of the temporomandibular joint? A study using geometric morphometrics on the skulls of wolves and domestic dogs. *Annals of Anatomy*, *214*, 53–62.
- Endo, M., Terajima, M., Goto, T. K., Tokumori, K., & Takahashi, I. (2011). Three-dimensional analysis of the temporomandibular joint and fossa-condyle relationship. *The Orthodontist*, *12*, 210–221.
- Ferrario, V. F., Sforza, C., Lovecchio, N., & Mian, F. (2005). Quantification of translational and gliding components in human temporomandibular joint during mouth opening. *Archives of Oral Biology*, *50*, 507–515.
- Gallo, L. M., Airoidi, G. B., Airoidi, R. L., & Palla, S. (1997). Description of mandibular finite helical axis pathways in asymptomatic subjects. *Journal of Dental Research*, *76*, 704–713.
- Gallo, L. M., Fushima, K., & Palla, S. (2000). Mandibular helical axis pathways during mastication. *Journal of Dental Research*, *79*, 1566–1572.
- Granados, J. I. (1979). The influence of the loss of teeth and attrition on the articular eminence. *Journal of Prosthetic Dentistry*, *42*, 78–85.
- Grant, P. G. (1973). Biomechanical significance of the instantaneous center of rotation: The human temporomandibular joint. *Journal of Biomechanics*, *6*, 109–113.
- Hinton, R. J. (1981). Changes in articular eminence morphology with dental function. *American Journal of Physical Anthropology*, *54*, 439–455.
- Hinton, R. J. (1983). Relationships between mandibular joint size and craniofacial size in human groups. *Archives of Oral Biology*, *28*, 37–43.
- Hinton, R. J., & Carlson, D. S. (1979). Temporal changes in human temporomandibular joint size and shape. *American Journal of Physical Anthropology*, *50*, 325–333.
- Hinton, R. J., & McNamara, J. A. (1984). Temporal bone adaptations in response to protrusive function in juvenile and young

- adult rhesus monkeys (*Macaca mulatta*). *European Journal of Orthodontics*, 6, 155–174.
- Hylander, W. L. (1977). An experimental analysis of temporomandibular joint reaction force in macaques. *American Journal of Physical Anthropology*, 51, 433–456.
- Hylander, W. L. (1979). Functional significance of primate mandibular form. *Journal of Morphology*, 160, 223–239.
- Hylander, W. L. (1988). Implication of in vivo experiments for interpreting the functional significance of “robust” australopithecine jaws. In F. E. Grine (Ed.), *The evolutionary history of the “robust” australopithecines* (pp. 55–83). Aldine de Gruyter.
- Hylander, W. L. (2006). Functional anatomy and biomechanics of the masticatory apparatus. In D. Laskin, C. Greene, & W. Hylander (Eds.), *Temporomandibular disorders: An evidence-based approach to diagnosis and treatment* (pp. 3–34). Quintessence Pub Co.
- Hylander, W. L. (2013). Functional links between canine height and jaw gape in catarrhines with special reference to early hominins. *American Journal of Physical Anthropology*, 150, 247–259.
- Hylander, W. L., & Bays, R. (1979). In vivo strain-gauge analysis of the squamosal-dentary joint reaction force during mastication and incisal biting in *Macaca mulatta* and *Macaca fascicularis*. *Archives of Oral Biology*, 24, 689–697.
- Jarvey, J. C., Low, B. S., Pappano, D. J., Bergman, T. J., & Beehner, J. C. (2018). Graminivory and fallback foods: Annual diet profile of geladas (*Theropithecus gelada*) living in the Simien Mountains National Park, Ethiopia. *International Journal of Primatology*, 39, 105–126.
- Jasinevicius, T. R., Pyle, M. A., Lalumandier, J. A., Nelson, S., Kohrs, K. J., Turp, J. C., & Sawyer, D. R. (2006). Asymmetry of the articular eminence in dentate and partially edentulous populations. *Cranio*, 24, 85–94.
- Klingenberg, C. P. (2011). MorphoJ: An integrated software package for geometric morphometrics. *Molecular Ecology Resources*, 11, 353–357.
- Koppe, T., Schöbel, S. L., Bärenklau, M., Bruchhaus, H., Jankauskas, R., & Kaduk, W. M. H. (2007). Factors affecting the variation in the adult temporomandibular joint of archaeological human populations. *Annals of Anatomy*, 189, 320–325.
- Kurita, H., Ohtsuka, A., Kobayashi, H., & Kurashina, K. (2000). Flattening of the articular eminence correlates with progressive internal derangement of the temporomandibular joint. *Dento Maxillo Facial Radiology*, 29, 277–279.
- Lambert, J. E., & Rothman, J. M. (2015). Fallback foods, optimal diets, and nutritional targets: Primate responses to varying food availability and quality. *Annual Review of Anthropology*, 44, 493–512.
- Lockwood, C. A., Lynch, J. M., & Kimbel, W. H. (2002). Quantifying temporal bone morphology of great apes and humans: An approach using geometric morphometrics. *Journal of Anatomy*, 201, 447–464.
- Marshall, A. J., Boyko, C. M., Feilen, K. L., Boyko, R. H., & Leighton, M. (2009). Defining fallback foods and assessing their importance in primate ecology and evolution. *American Journal of Physical Anthropology*, 140, 603–614.
- Matsuka, Y., Iijima, T., Suzuki, K., Kuboki, T., & Yamashita, A. (1998). Macroscopic osseous changes in the temporomandibular joint related to dental attrition in the Japanese macaque skull. *Journal of Oral Rehabilitation*, 25, 687–693.
- Mitchell, D. R. (2019). The anatomy of a crushing bite: The specialised cranial mechanics of a giant extinct kangaroo. *PLoS One*, 14(9), e0221287.
- Mitchell, D. R., Kirchoff, C. A., Cooke, S. B., & Terhune, C. E. (2021). Bolstering geometric morphometrics sample sizes with damaged and pathologic specimens: Is near enough good enough? *Journal of Anatomy*, 238, 1444–1455.
- Miyawaki, S., Ohkochi, N., Kawakami, T., & Sugimura, M. (2000). Effect of food size on the movement of the mandibular first molars and condyles during deliberate unilateral mastication in humans. *Journal of Dental Research*, 79, 1525–1531.
- Miyawaki, S., Tanimoto, Y., Kawakami, T., Sugimura, M., & Takano-Yamamoto, T. (2001). Motion of the human mandibular condyle during mastication. *Journal of Dental Research*, 80, 437–442.
- Moffett, B. C., Askew, H. C., McCabe, J. B., & Johnson, L. C. (1964). Articular remodeling in adult human temporomandibular joint. *The American Journal of Anatomy*, 115, 119–141.
- Malenky, R. K., & Stiles, E. W. (1991). Distribution of terrestrial herbaceous vegetation and its consumption by *Pan paniscus* in the Lomako Forest, Zaire. *American Journal of Primatology*, 23, 153–169.
- Malenky, R. K., & Wrangham, R. W. (1994). A quantitative comparison of terrestrial herbaceous food consumption by *Pan paniscus* in the Lomako Forest, Zaire, and *Pan troglodytes* in the Kibale Forest, Uganda. *American Journal of Primatology*, 32, 1–12.
- Nickel, J. C., McLachlan, K. R., & Smith, D. M. (1988). Eminence development of the postnatal human temporomandibular joint. *Journal of Dental Research*, 67, 896–902.
- Öberg, T., Carlsson, G. E., & Fajers, C.-M. (1971). The temporomandibular joint: A morphologic study on a human autopsy material. *Acta Odontologica Scandinavica*, 29, 349–384.
- Osborn, J., & Baragar, F. (1992). Predicted and observed shapes of human mandibular condyles. *Journal of Biomechanics*, 25, 967–974.
- Plavcan J. M. (1990). Sexual dimorphism in the dentition of extant anthropoid primates. PhD Dissertation, Duke University.
- Plavcan, J. M. (2001). Sexual dimorphism in primate evolution. *American Journal of Physical Anthropology*, 44, 25–53.
- Plavcan, J. M., van Schaik, C. P., & Kappeler, P. M. (1995). Competition, coalitions and canine size in primates. *Journal of Human Evolution*, 28, 245–276.
- R Core Team. (2021). *R: A language and environment for statistical computing*. R Foundation for Statistical Computing. Available from: <https://www.R-project.org/>
- Richards, L. (1988). Degenerative changes in the temporomandibular joint in two Australian aboriginal populations. *Journal of Dental Research*, 67, 1529–1533.
- Richards, L. C., & Brown, T. (1981). Dental attrition and degenerative arthritis of the temporomandibular joint. *Journal of Oral Rehabilitation*, 8, 293–307.
- Robinson, C., & Terhune, C. E. (2017). Error in geometric morphometric data collection: Combining data from multiple sources. *American Journal of Physical Anthropology*, 164, 62–75.
- Rohlf, F. J., & Corti, M. (2000). Use of two-block partial least-squares to study covariation in shape. *Systematic Biology*, 49, 740–753.
- Romero, A. N., Mitchell, D. R., Cooke, S. B., Kirchoff, C. A., & Terhune, C. E. (2022). Craniofacial fluctuating asymmetry in gorillas, chimpanzees, and macaques. *American Journal of*

- Physical Anthropology*, 177, 286–299. <https://doi.org/10.1002/ajpa.24432>
- Ross, C. F., & Iriarte-Diaz, J. (2014). What does feeding system morphology tell us about feeding? *Evolutionary Anthropology*, 23, 105–120.
- Ross, C. F., Iriarte-Diaz, J., & Nunn, C. L. (2012). Innovative approaches to the relationship between diet and mandibular morphology in primates. *International Journal of Primatology*, 33, 632–660.
- Serckx, A., Kühl, H. S., Beudels-Jamar, R. C., Poncin, P., Bastin, J. F., & Huynen, M. C. (2015). Feeding ecology of bonobos living in forest-savannah mosaics: Diet seasonal variation and importance of fall-back foods. *American Journal of Primatology*, 77, 948–962.
- Shearer, B. M., Cooke, S. B., Halenar, L. B., Reber, S. L., Plummer, J. E., Delson, E., & Tallman, M. (2017). Evaluating causes of error in landmark-based data collection using scanners. *PLoS One*, 12(11), e0187452.
- Smith, R. J., Petersen, C. E., & Gipe, D. P. (1983). Size and shape of the mandibular condyle in primates. *Journal of Morphology*, 177, 59–68.
- Taylor, A. B. (2005). A comparative analysis of temporomandibular joint morphology in the African apes. *Journal of Human Evolution*, 48, 555–574.
- Taylor, A. B., Terhune, C. E., Toler, M., Holmes, M., Ross, C. F., & Vinyard, C. J. (2018). Jaw-muscle fiber architecture and leverage in the hard-object feeding Sooty Mangabey are not structured to facilitate relatively large bite forces compared to other papionins. *The Anatomical Record*, 301, 325–342.
- Taylor, A. B., Yuan, T., Ross, C. F., & Vinyard, C. J. (2015). Jaw-muscle force and excursion scale with negative allometry in platyrrhine primates. *American Journal of Physical Anthropology*, 158, 242–256.
- Terhune, C. E. (2010). The temporomandibular joint in anthropoid primates: Functional, allometric, and phylogenetic influences. PhD Dissertation, Arizona State University.
- Terhune, C. E. (2011a). Dietary correlates of temporomandibular joint morphology in New World primates. *Journal of Human Evolution*, 61, 583–596.
- Terhune, C. E. (2011b). Modeling the biomechanics of articular eminence function in anthropoid primates. *Journal of Anatomy*, 219, 551–564.
- Terhune, C. E. (2013a). Dietary correlates of temporomandibular joint morphology in the great apes. *American Journal of Physical Anthropology*, 150, 260–272.
- Terhune, C. E. (2013b). How effective are geometric morphometric techniques for assessing functional shape variation? An example from the great ape temporomandibular joint. *The Anatomical Record*, 296, 1264–1282.
- Terhune, C. E. (2017). Revisiting size and scaling in the anthropoid temporomandibular joint. *Zoology*, 124, 73–94.
- Terhune, C. E., Cooke, S. B., & Otarola-Castillo, E. (2015). Form and function in the platyrrhine skull: A three-dimensional analysis of dental and TMJ morphology. *The Anatomical Record*, 298, 29–47.
- Terhune, C. E., Hylander, W. L., Vinyard, C. J., & Taylor, A. B. (2015). Jaw-muscle architecture and mandibular morphology influence relative maximum jaw gapes in the sexually dimorphic *Macaca fascicularis*. *Journal of Human Evolution*, 82, 145–158.
- Turp, J. C., Greene, C. S., & Strub, J. R. (2008). Dental occlusion: A critical reflection on past, present and future concepts. *Journal of Oral Rehabilitation*, 35, 446–453.
- Tutin, C. E. G., & Fernandez, M. (1993). Composition of the diet of chimpanzees and comparisons with that of sympatric lowland gorillas in the Lope Reserve, Gabon. *American Journal of Primatology*, 30, 195–211.
- Vinyard, C. J. (1999). Temporomandibular joint morphology and function in strepsirhine and eocene primates (*Otolemur crassicaudatus*). PhD Dissertation, Northwestern University.
- Vinyard, C. J. (2008). Putting shape to work: Making functional interpretations of masticatory apparatus shapes in primates. In *Primate craniofacial function and biology* (pp. 357–385). Springer.
- Vinyard, C. J., Taylor, A. B., Teaford, M. F., Glander, K. E., Ravosa, M. J., Rossie, J. B., Ryan, T. M., & Williams, S. H. (2011). Are we looking for loads in all the right places? New research directions for studying the masticatory apparatus of New World monkeys. *The Anatomical Record*, 294, 2140–2157.
- Vinyard, C. J., Wall, C. E., Williams, S. H., & Hylander, W. L. (2003). Comparative functional analysis of skull morphology of tree-gouging primates. *American Journal of Physical Anthropology*, 120, 153–170.
- Vinyard, C. J., Wall, C. E., Williams, S. H., & Hylander, W. L. (2008). Patterns of variation across primates in jaw-muscle electromyography during mastication. *American Zoologist*, 48, 294–311.
- Wainwright, P. C., Alfaro, M. E., Bolnick, D. I., & Hulseay, C. D. (2005). Many-to-one mapping of form to function: A general principle in organismal design? *Integrative and Comparative Biology*, 45, 256–262.
- Wall, C. E. (1995). Form and function of the temporomandibular joint in anthropoid primates. PhD Dissertation, State University of New York at Stony Brook.
- Wall, C. E. (1997). The expanded mandibular condyle of the Megaladapidae. *American Journal of Physical Anthropology*, 103, 263–276.
- Wall, C. E. (1999). A model of temporomandibular joint function in anthropoid primates based on condylar movements during mastication. *American Journal of Physical Anthropology*, 109, 67–88.
- Williamson, E. A., Tutin, C. E. G., Rogers, M. E., & Fernandez, M. (1990). Composition of the diet of lowland gorillas at Lope in Gabon. *American Journal of Primatology*, 21, 265–277.
- Wiley, D. F., Amenta, N., Alcantara, D. A., Ghosh, D., Kil, Y. J., Delson, E., Harcourt-Smith, W., Rohlf, F. J., St John, K., & Hamann, B. (2005). Evolutionary morphing. VIS 05, IEEE Visualization, 431–438.
- Yamada, K., Tsuruta, A., Hanada, K., & Hayashi, T. (2004). Morphology of the articular eminence in temporomandibular joints and condylar bone change. *Journal of Oral Rehabilitation*, 31, 438–444.

## SUPPORTING INFORMATION

Additional supporting information may be found in the online version of the article at the publisher's website.

**How to cite this article:** Terhune, C. E., Mitchell, D. R., Cooke, S. B., Kirchhoff, C. A., & Massey, J. S. (2022). Temporomandibular joint shape in anthropoid primates varies widely and is patterned by size and phylogeny. *The Anatomical Record*, 305(9), 2227–2248. <https://doi.org/10.1002/ar.24886>